

UNCLASSIFIED

SECURITY CLASSIFICATION OF THIS PAGE (When Data Entered)

2

REPORT DOCUMENTATION PAGE

READ INSTRUCTIONS BEFORE COMPLETING FORM

1. REPORT NUMBER ARO 19684.2-GS		2. GOVT ACCESSION NO. N/A	3. RECIPIENT'S CATALOG NUMBER N/A
4. TITLE (and Subtitle) Genesis of Major Dust Storms in West Africa During the Summer of 1974		5. TYPE OF REPORT & PERIOD COVERED Technical Report	
7. AUTHOR(s) M. Estoque, J. Fernandez-Partagas, D. M. Helgren and J. M. Prospero		6. PERFORMING ORG. REPORT NUMBER	
9. PERFORMING ORGANIZATION NAME AND ADDRESS University of Miami Miami, Florida 33149-1098		8. CONTRACT OR GRANT NUMBER(s) DAAG29-83-K-0082	
11. CONTROLLING OFFICE NAME AND ADDRESS U. S. Army Research Office Post Office Box 12211 Research Triangle Park, NC 27709		10. PROGRAM ELEMENT, PROJECT, TASK AREA & WORK UNIT NUMBERS	
14. MONITORING AGENCY NAME & ADDRESS (if different from Controlling Office)		12. REPORT DATE January, 1986	
		13. NUMBER OF PAGES	
		15. SECURITY CLASS. (of this report) Unclassified	
		15a. DECLASSIFICATION/DOWNGRADING SCHEDULE	

16. DISTRIBUTION STATEMENT (of this Report)
Approved for public release; distribution unlimited.

DTIC ELECTE
MAR 20 1986
S B D

17. DISTRIBUTION STATEMENT (of the abstract entered in Block 20, if different from Report)
NA

18. SUPPLEMENTARY NOTES
The view, opinions, and/or findings contained in this report are those of the author(s) and should not be construed as an official Department of the Army position, policy, or decision, unless so designated by other documentation.

19. KEY WORDS (Continue on reverse side if necessary and identify by block number)
Dust Storms Surface Cyclones
West Africa Cyclones
Dust Clouds Dust Generation
Flow Patterns

20. ABSTRACT (Continue on reverse side if necessary and identify by block number)
The occurrence of major dust clouds over the western Sahara is associated with several characteristic features of the large scale synoptic conditions, including the isallobaric pattern as well as the flow patterns at the 850-700 mb layer and the surface. A necessary ingredient for the occurrence of dust appears to be the existence of a well developed and intense surface cyclone along the ITF south of the dust

AD-A165 457

DTIC FILE COPY

86 3 18 328

20. ABSTRACT CONTINUED

source region. These three features are incorporated in three synoptic models for dust generation. The models are: the general model (GM), the model without a trough (NTM) and the model with a trough (TM). Conditions resembling those in the TM appear to be the ones most frequently observed during dust episodes in GATE.



Accession For	
NTM	<input checked="" type="checkbox"/>
DTM	<input type="checkbox"/>
General model	<input type="checkbox"/>
Justification	
By	
Date	
Availability Codes	
Dist	Special
A-1	

GENESIS OF MAJOR DUST STORMS IN WEST AFRICA DURING THE SUMMER OF 1974

TECHNICAL REPORT

M. ESTOQUE, J. FERNANDEZ-PARTAGAS, D.M. HELGREN AND J.M. PROSPERO

JANUARY, 1986

U.S. ARMY RESEARCH OFFICE

CONTRACT NO. DAAG29-83-K-0082

UNIVERSITY OF MIAMI
ROSENSTIEL SCHOOL OF MARINE AND ATMOSPHERIC SCIENCE
MIAMI, FLORIDA 33149-1098

APPROVED FOR PUBLIC RELEASE;
DISTRIBUTION UNLIMITED

THE VIEW, OPINIONS, AND/OR FINDINGS CONTAINED IN THIS REPORT ARE THOSE OF THE AUTHOR(S) AND SHOULD NOT BE CONSTRUED AS AN OFFICIAL DEPARTMENT OF THE ARMY POSITION, POLICY, OR DECISION, UNLESS SO DESIGNATED BY OTHER DOCUMENTATION.

1. Introduction

The generation of large scale dust episodes over arid and semiarid landscapes requires two atmospheric conditions: 1) surface winds sufficiently strong to cause erosion and, 2) strong vertical transport to carry the dust into the troposphere. According to Kalu (1979), a wind speed of at least 30 knots (15 m/sec) is required in order to forecast the generation of dust clouds from the Bilma - Faya Largeau source area. On the other hand, Morales (1979) has indicated that the threshold speed for raising soil dust into the air is about 12 knots (6 m/sec) from a site in the Sudan. This low value is based on reports from only one station during a one-month period (April 1973) but it is in line with some other synoptic reports of dust being raised by 17-knot (9 m/sec) winds (Morales, 1979). The most extensive study of dust storm generation conditions in North Africa is that of Fernandez-Partagas et al. (1986); using meteorological observations from 8 stations in northern and western Africa for the period July 1 to August 15, 1974, they found a mean threshold value of 16 knots (8 m/sec). The threshold speed depends on soil and surface sediment attributes as well as other local environmental variables so that the threshold speed could change with location and with time (Gillette, 1979). In the south western United States, the threshold velocity is a function of threshold friction speed, particle sizes, soil type, surface characteristics and the degree to which the soil is disturbed (Gillette, 1979).

Vertical transport of dust can occur under conditions of unstable thermal stratification because of the development of intense turbulent eddies ranging in size from small scale to convective scale. These eddies can transport dust from the surface layer upward into the middle and upper troposphere.

In addition, the upward transport of dust also can result from large-scale synoptic upward motions. For example, dust storms in China are generated as a rapidly moving cold fronts overtake slower fronts (Avila, 1984; Merrill et al., 1985).

While it is clear that the genesis and subsequent transport of dust clouds in the atmosphere is dependent on many meteorological variables, there have been no detailed and systematic studies of the synoptic conditions associated with major dust events. Most reports in the literature consist of isolated case studies or of a generalized discussion of the meteorology of such events.

The principal objective of this study is to investigate the meteorological settings of major dust storms occurring in the western Sahara. Previous studies (Delany et al., 1967; Carlson and Prospero, 1972; Prospero and Carlson, 1972; Prospero, 1979; Prospero et al., 1979; Prospero, 1981; Prospero and Nees, 1977, 1986; Jaenicke, 1979; Jaenicke and Schutz, 1978; Schutz et al., 1981) have shown that large numbers of dust storms emerge from the west coast of Africa during much of the year. During the summer months, dust from these storms frequently impacts the entire tropical and subtropical North Atlantic (Prospero and Nees, 1977, 1986) as far North as Miami (Carder et al. 1986; Prospero, Nees and Uematsu, 1985) and Bermuda (Chen and Duce, 1983). For this reason, in

this study we focus on summer dust storms.

During the summer, over West Africa, there are two types of synoptic disturbances that are characterized by strong surface winds and unstable thermal stratification. One of these types is an intensifying anticyclone over northwest Africa. The southeastern periphery of this anticyclone is usually characterized by strong winds and unstable conditions. This type of flow pattern is most common in winter and spring (Dubief, 1953, 1959, 1979; Lee, 1983) but it also occurs in the summer, although usually with less intensity. The other type of dust-related synoptic flow pattern in the summer is characterized by a cyclonic disturbance (Dubief, 1979). This disturbance develops at the surface along the Intertropical Front (ITF) and generally propagates westward. The surface cyclone is generally reflected at upper levels as a wave trough, which may be responsible for the typical flow pattern observed at 700 mb during Saharan dust outbreaks as they pass off the coast of West Africa (Carlson and Prospero, 1972). Presumably, there are other types of synoptic situations which might also trigger large scale dust episodes. However, the sparsity of meteorological observations in the Sahara, especially upper air observations, has made it difficult to study meteorological events in detail.

This study focuses on the summer of 1974, which coincided with the Global Atmospheric Research Program (GARP) Atlantic Tropical Experiment (GATE). GATE provided us with a large meteorological data set and improved coverage of North Africa via the SMS-1 geostationary satellite.

Specific objectives are:

- (1) To provide a detailed description of the synoptic conditions for this period;
- (2) To identify the synoptic flow patterns that are associated with the occurrence of large scale dust clouds during this period; and
- (3) To develop empirical models of the synoptic flow patterns that generate large scale dust clouds.

2. Data and analyses

The meteorological data analyzed in this study consist of standard observations at the surface as well as upper air observations from radiosondes and pilot balloons. In addition, we used some upper air data from aircraft and satellites. Meteorological data were read from tapes obtained from the National Climatic Center at Asheville, North Carolina.

Wind data for 1200 GMT were plotted on daily maps for the surface and at several levels of the atmosphere: 850 mb (about 1.5 km), 700 mb (about 3 km), 500 mb (about 6 km), and 300 mb (about 10 km). Dust-related phenomena (haze, dust in the air but not rising from the ground, dust rising from the ground, dust storms) were also plotted on the surface wind maps for reference in determining the occurrence of dust in the atmosphere (Gates, 1965). Surface pressure values were also plotted on separate maps.

Surface and upper level winds were analyzed using conventional streamline analysis techniques. Cyclonic and anticyclonic patterns were inferred from streamline configurations. Space and time continuity from one map to another were maintained as much as possible. Analysis was often difficult because of the sparseness of wind data over very large areas of North Africa, especially in the Western Sahara, the area of greatest interest to us. Wind speed analysis (isotachs) could not be done because of the few stations and the frequently conflicting wind speed observations at neighboring stations, especially for surface observations.

In addition to the surface wind analysis, we also constructed corresponding maps of 24-hour local pressure change (isallobaric maps) using 2 mb contour intervals. These maps enable us to determine the regions of pressure change and the amplitude of changes. The magnitude, extent, movement and orientation of these areas are important because they are related to temporal changes in the wind field.

The locations of dust storms over the western Sahara were identified from SMS-1 infra-red (IR) satellite images. During GATE the SMS-1 geosynchronous satellite was moved to a more easterly position near 0°N, 45°W which permitted observations of North Africa to about 20°E. In the IR, major dust events can usually be identified because of the temperature contrast between the dust cloud and the hot desert surface; in a typical image, the dust cloud is gray and the desert surface black. It is usually possible to make a clear distinction between dust and water clouds; the latter are generally colder (whiter) and they have smaller scale structural features which display greater short-term temporal variability. However, in areas where cloud cover is relatively high, it is not possible to consistently identify dust storm events. This problem was especially severe in the region south of about 20°N, along the ITF. It is for this reason that we confined our study to the western Sahara.

We focussed on those dust events that could be identified at the time of their inception. Because SMS-1 imagery was available at 30 minute intervals, it was relatively easy to establish the time and location of storm genesis by perusing the SMS-1 archive. Because of the synoptic-scale nature of this work, we incorporated only major dust events - storms that extended over at least several degrees of latitude and longitude. In general, major storms were obvious events; there was only one case where there was any ambiguity about the classification of a storm as major or minor. For the purpose of this study, it was not necessary to have accurate navigation of the image. Consequently, the outline of the storm and its position were determined by direct tracings from photographs and the fitting of navigation grid overlays. The dust storm outlines were then redrawn on the maps used for wind and pressure analyses in order to determine the relationships between these patterns and the wind and pressure fields. These products serve as the foundation of this study.

3. Results

a. Environmental Setting of Major Western Sahara Dust Storms

The base period of our study is July 1974. The major dust storms during this time developed in the hyperarid landscapes of southern

Algeria, northern Mali and eastern Mauritania (Fig. 1). This region, west and southwest of the Ahaggar massif, is dominated by wide sandy and gravelly plains interrupted by low escarpments, dry lakebeds and rows of both small and large dunes. Vegetation is limited to grasses and hardy shrubs with many areas having no large flowering plants at all. This part of the Sahara is one of the most desolate and, despite its large size, there are few settlements and few travelers. In Fig. 2 we show the outlines of all nine newly-generated major dust storms observed on satellite photographs during July: July 2, 3, 8, 12, 21, 22, 23, 28, and 29. Most dust clouds are in the form of elongated plumes which are generally oriented from northeast to southwest. A typical plume is about 1000 km long and 200 km wide. The longest plume (about 1500 km long) occurred on July 8; short plumes (about 700 km long) occurred on July 12 and 21.

The synoptic flow patterns associated with these dust events have the following characteristics:

- (1) A persistent east-west low tropospheric trough that lies roughly along 20°N latitude which corresponds to the ITF.
- (2) A well-defined and extremely persistent anticyclonic pattern over North Africa at all levels from the surface up to the 300-mb level.
- (3) A north-south trough frequently found over West Africa between 10°W meridian and the Atlantic coast. At the intersection of this trough and the ITF, cyclonic circulations are almost invariably observed. These cyclonic circulations are generally confined to the lowest tropospheric layers and seldom extend above the 850 mb level.
- (4) Low-latitude wave disturbances generally propagating westward along the ITF and best defined at middle levels (700 and 500 mb).

The meteorological conditions in July 1974 appear to be generally consistent with climatological mean features. Items (1) to (3) above are similar to corresponding features in the climatological maps (Figs. 3 to 5) taken from Thompson (1965). There are some indications, however, that the anticyclonic conditions over North Africa were somewhat more pronounced in July 1974 relative to the mean climatological conditions. At several stations in tropical and subtropical Africa, surface pressure in July 1974 were found to be 1 to 2 mb higher than normal. Only at one station in tropical Central Africa was the surface pressure observed to be about 2 mb lower than normal. The upward extension of the anticyclonic pattern over North Africa in July 1974 is also in general agreement with the corresponding extensions at the 850 and 700 mb levels shown in Figs. 4 to 5. However, a close comparison with climatological maps is not appropriate because we used streamline analysis whereas the climatological maps present isobaric contour heights.

The presence of the ITCZ trough and the tendency for a north-south trough to develop over West Africa in July 1974 are consistent with the climatological conditions depicted in Figs. 3 and 4 for the surface and 850 mb respectively. The ITCZ in July 1974 was generally located near its surface climatological position, except perhaps between 0° and 10°W where

its location was perhaps a little to the south.

In order to complete the description of the flow patterns for July, we have plotted the daily positions of all surface cyclone centers and 700 mb troughs that occurred during the month (Figs. 6 and 7). These troughs are of interest because, according to Carlson and Prospero (1972), over the ocean, dust clouds are often found behind the 700 mb troughs. In Figures 6 and 7, we have also indicated the cyclone centers and troughs that are accompanied by the occurrence of dust clouds. The cyclone centers tend to cluster near 20°N (Fig. 6), which is the mean position of the ITF in July. There are nine cyclone centers that are associated with dust clouds, all of these centers are located within 10° of longitude from the Ahaggar massif. The 700 mb troughs tend to cluster around two regions: 1) near the West African coast and 2) in the region between 2°E and 12°E . The locations of the 700 mb troughs on days of dust occurrences are not as tightly clustered as the locations of cyclone centers.

As stated earlier, previous studies have suggested that there is an association between cyclones and dust storms. This also appears to be the case for dust clouds in July 1974. This may be seen in Figs. 8 to 16 which show the surface streamline maps for the 9 days of dust occurrences; the dust plumes are superimposed on each of the 9 streamline maps. Dust events generally occurred when a cyclone center was in the vicinity of the source and located either to the south or the east.

L. Synoptic Composites of Dust Storm Events

To more clearly show the association of dust events with cyclonic centers, we prepared a composite dust plume by referencing the position of each plume to that of the cyclonic center (Fig. 17). The composite map was made by first plotting the mean geographical position of the 9 cyclone centers on the map and then drawing the outlines of the dust clouds at a position relative to that of the mean cyclone center position. The dust storms are generally located in an area northwest of the cyclone center. The long axis of the dust cloud is often oriented from northeast to southwest. Using the dust outlines in Fig. 17, we determined a mean dust pattern by graphical addition. We arbitrarily assumed that the outline of a particular dust plume has a dust concentration value of one unit and that the area enclosed has dust concentration values between one and two. Finally, we defined the outline of the composite dust cloud as the area enclosed by the dust concentration isoline having the average value. The result is shown in Fig. 18. On the same map we superimposed the corresponding composite flow in the 850 to 700 mb layer for the 9 days of dust occurrences. Note that the general orientation of the dust plume is parallel to that of the composite 850-700 mb flow. There is no clear indication of a trough in this flow pattern. This is surprising because, according to the model described by Carlson and Prospero (1972), dust clouds were found to be associated with the area to the east of a 700 mb trough. The apparent lack of agreement between our composite flow pattern for July 1974 and Carlson-Prospero model may be related to the fact that the latter model was based on observations along the West African coast and over the eastern Atlantic; apparently it is not applicable over the interior of Africa.

c. Flow Field Characteristics

An examination of the individual maps that were used to make our composite suggested that the flow patterns could be divided roughly into two types. One type is characterized by a cyclonic curvature in the 850 - 700 layer flow pattern; for the other one, the curvature is anticyclonic. A composite of the flow patterns and the dust plumes corresponding to the anticyclonic days (July 2, 3, 12, 28, and 29) is shown in Fig. 19. The corresponding composites for the cyclonic days (July 8, 21, 22, and 23) are shown in Fig. 20. There is little difference between the two composites for the dust plumes. The only significant difference appears to be a tendency for the anticyclonic dust plume to curve cyclonically around the center of the surface cyclone. Since the number of cases used in making the composites is limited, it is unclear whether this tendency is a universal characteristics of anticyclonic flow patterns. In Figure 20, the cyclonic flow pattern is characterized by a trough. As noted, this type of flow pattern is different from the model described by Carlson and Prospero (1972) wherein the dust plume is located behind the trough; in Fig. 20, the dust plume is ahead of the trough.

d. Isallobaric Relationships

There appears to be a relationship between the 24 hour local pressure (isallobaric patterns) and dust occurrences. To display this relationship, we developed composites with respect to the surface cyclone center in the same way as for dust plumes (Fig. 21). The occurrence of dust plumes appears to be associated with negative pressure changes to the southwest of the center of the dust plume and with significant pressure rises farther to the northwest. The isallobaric patterns imply large increases in the geostrophic wind west of the cyclone center. The increase in the wind is presumably a contributing cause of the observed dust events in that area.

We prepared composites of two subsets of isallobaric patterns, one for dust storms during anticyclonic flow conditions (Fig. 22) and one for cyclonic conditions (Fig. 23). There is a large difference in the isallobaric patterns for these two situations. The anticyclonic flow composite is dominated by large pressure rises primarily to the west and northwest of the center. This pattern implies an intensification of the anticyclone to the northwest and a concomittant increase in the wind west of the cyclone center. The cyclonic flow composite, on the other hand, is dominated by large pressure falls southwest of the cyclone center and an area of pressure rises north of the center. This pattern suggests that the wind speed increase is due to the intensification of both the surface cyclone and the anticyclone.

In summary, the dust generation in the anticyclonic flow subset is associated primarily with the intensification of an anticyclone to the northwest; the generation in the cyclonic flow subset is associated with the intensification of the surface cyclone to the southwest as well as with the intensification of the anticyclone to the north.

e. Surface Temperature

There is some evidence that the intensification of the anticyclone associated with the dust episodes might be related to temporal changes in the surface temperature. Fig. 24 is a composite of 24 hr surface temperature changes for the region to the north and northeast of the surface cyclone and for all days showing dust plumes; however, only five of the nine dust-plume days contribute significantly to the composite. The composite shows some cooling to the northeast of the cyclone. The cooling coincides quite well with pressure rises in the same area (Fig. 21).

The composite of 24 hr surface temperature changes was not extended to the areas of pressure rises to the northwest of the surface cyclone because neighboring stations in that area tend to show temporal temperature changes that do not agree with one another. Fig. 25 is an example of the disagreement between the 1200 GMT temperature records at two stations - Marrakech (altitude 466m) and Ouarzazate (altitude 1136m) which are located only about 150 km apart. Marrakech (60230) is located on the northwestern slopes of the Atlas Mountains while Ouarzazate (60265) is located at high ground just to the east of the mountain tops. In general, temperature maxima and minima do not occur on the same days at both stations. This suggests that mountain effects complicate the temperature behaviour at each station.

f. Pressure Gradient

Finally, we examined the relationship between dust storm genesis and the strength of the pressure gradient in the vicinity of the composite dust plume. The pressure gradient used in this examination was the one estimated over a distance of 10° latitude to the north of the cyclonic center. Table 1 shows a listing of the strength of the pressure gradient arranged so that the strongest is listed first (No.1) while the weakest is listed last. Columns indicating the date of observation, cyclone location and dust occurrence are also included. Note that most cases of dust occurrence are related to pressure gradients of at least 6 mb per 10° latitude. However, it is surprising to see that about an equal number of cases of at least 6 mb per 10° latitude had no dust occurrences. However in most of the latter cases, the cyclone centers are located far from the source region. The mean gradient for 9 dust cases is equal to 7.3 mb per 10° latitude which - at 25° North latitude - corresponds to a geostrophic wind speed of about 17 knots (8.5 m/sec). The mean gradient for 26 non dust cases is 4.8 mb per 10° latitude; the equivalent geostrophic wind is about 11 knots (5.5 m/sec).

4. Models of Dust Storm Genesis

On the basis of the discussions in the previous sections, we can postulate three empirical models of the synoptic conditions associated with the genesis of major dust storms. One of these models, the general model (GM), represents a synthesis of all the occurrences of dust clouds in July, 1974. The other two are special cases of the GM: a model with a trough (TM) and a model without a trough (no trough, NTM). Each of these

models involves the specification of the flow pattern in the 850-700 mb layer, the pattern of the 24-hour surface pressure changes, the geographical position of the center of an associated surface cyclone, and the pattern of the dust plume. The relationships between these features of the atmosphere and the dust plume are summarized in Figs. 26 (GM), 27 (TM), and 28 (NTM) which are graphical representations of the three models. In this section, we will assess the applicability of these models by using dust events that occurred outside the July study period. The data consist of maps based on observations during dust storms that occurred on eight separate days in June, August, and September, 1974: June 28, June 29, June 30, August 2, August 8, August 9, August 25 and September 3. These events along with the nine that occurred in July constitute all the major dust storms that could be unambiguously identified in satellite imagery.

June 28, 1974 case (Fig. 29). Although having its own peculiarities, this case appears to resemble the GM (Fig. 26). The case does not seem to correspond with the NTM (Fig. 28) because the 850 - 700 mb flow is cyclonic on June 28 instead of anticyclonic as in that model; furthermore, falling pressure is located to the northeast of the surface cyclone in the NTM, whereas rising pressure is observed in this individual case. The intense falling pressure center to the southwest of the surface cyclone suggested by the TM (Fig. 27) is not observed in the June 28, 1974 individual case.

June 29, 1974 (Fig. 30). This case appears to fit the TM (Fig. 27) better than the other models. The presence of cyclonic curvature in the 850-700 mb flow definitely does not correspond to the NTM. Because of the fairly intense falling pressure center, this case does not conform to the GM which specified a weak center.

June 30, 1974 (Fig. 31). The position of the plume of this particular case does not fit the composited position in the models. The plume is located to the northeast of the surface cyclone and not to the north and northwest as suggested by the models. Aside from this difference, the 850 - 700 mb mean flow and the 24 hr pressure change distribution is similar to that in the TM (Fig. 27).

August 2, 1974 (Fig. 32). This particular case resembles the NTM (Fig. 28). The resemblance is mainly due to the anticyclonic turning of the 850 - 700 mb mean flow and, to a lesser extent, to a similar distribution in the 24 hr pressure pattern. The fit with the other models is not good because the other models show pressure rises to the north of the surface center and of the dust plume; these rises are not observed in this particular case.

August 8, 1974 (Fig. 33). This event does not fit any of the models. The plume is embedded in a northerly 850-700 mb mean flow and it is located to the northeast of the surface cyclone. No such patterns are suggested by any of the models.

August 9, 1974 (Fig. 34). This case resembles the TM (Fig. 27). The lack of anticyclonic turning in the 850 - 700 mb mean flow precludes

classification as an NTM. In this case there is an intense center of falling pressure to the west of the surface cyclone. This strong center contrasts with the weak center specified in the GM and places it closer to the TM than to the other models.

August 25, 1974 (Fig. 35). This case fits the TM (Fig. 27). Because of the marked cyclonic curvature observed in the 850 - 700 mb mean flow, this case cannot be classified as NTM. Because of the fairly large pressure decrease to the west of the surface cyclone, it does not qualify for the GM which calls for weak pressure drops.

September 3, 1974 (Fig. 36). This case fits the TM (Fig. 27). The presence of some cyclonic curvature in the 850 - 700 mb mean flow over the surface cyclone and absence of curvature in the plume area are factors favoring this classification. Other factors are the presence of pressure rises to the north of the plume and the intensity of the rises and falls.

In summary, we conclude that, seven of the eight test cases can be characterized by one of the models developed on the basis of July 1974 data. Five of the cases appear to fit the model with a trough (Fig. 27) better than the other models. Thus it appears that the conditions described by the TM occur more frequently than those of the other models.

5. Dust occurrences in relation to pressure gradients.

Two critically important factors in dust storm genesis are the wind speed and the existence of dust sources. In temperate latitudes, the wind speed is related to the horizontal pressure gradient through the geostrophic wind equation. Therefore, to the first order the pressure gradient can be substituted for the wind speed. We have examined quantitatively the relationship between the occurrence of dust plumes and these two factors. The results are discussed in this section.

To assess the importance of the horizontal pressure gradient as a factor in the generation of dust clouds, we examined first the time series of the daily values of the surface pressure at two points: 30°N latitude, 0° longitude and 20°N latitude, 0° longitude. These locations were selected because the pressure gradient between them represents the east-west wind speed component across the major dust source region. The time series incorporates data for the period July 1, 1974 to August 15, 1974. The surface pressures at these two locations are shown in Fig. 37. Also shown in the diagram is the pressure difference (northern pressure minus southern pressure) and the corresponding east-west component of the geostrophic wind speed. The days on which dust clouds were observed are indicated by dashed lines. There are three days (July 1, 11, 21) when the pressure difference between the two points exceeded 8 mb. The large pressure differences are associated by rises in pressure over the northern region and decreases in pressure over the southern region; this situation corresponds to the occurrence of an anticyclone in the north and a cyclone to the south. As expected, dust clouds were generated on these days or the days following these maxima in pressure differences. There were six other days on which dust clouds occurred with smaller pressure differences. Two of these days had a rather small pressure difference of 4 mb. These data suggest that a pressure difference of more than 4 mb will usually result in the generation of major dust events.

We next investigated the relationship between the location of cyclones and their proximity to the location of major dust events. Figure 38 shows the relative location of the cyclone center at the time that a major dust storm occurred. The location is specified in terms of the longitudinal distance of the cyclone center from the longitude (0°) of the major dust source region. Using the longitudinal distance and the pressure difference (pressure at 10 degrees to the north of the center minus pressure at the cyclone center) as abscissa and ordinate, respectively, we plotted points corresponding to cyclones for each day in the time series. Cyclone cases associated with dust occurrences noted here are indicated by crosses (X); cyclones that were not associated with dust events are indicated by dots. The resulting scatter diagram (Fig. 38) reveals two features. First, most points associated with strong pressure gradients and cyclones in the vicinity of 0° longitude correspond to days when a major dust storm occurred. Second, major dust storms did not occur on days with strong pressure gradients when the cyclone centers were far from 0° longitude. The data points for dust storm events are relatively tightly clustered while those for non-dust storm days fall predominantly outside the cluster. Hence, the diagram can be used to predict major dust events if the location of the cyclone center and the pressure gradient to the north of the cyclone are known.

6. Concluding Comments.

The primary objective of this investigation is to determine the synoptic conditions that accompany large scale dust storm genesis over the western Sahara during the summer of 1974. The location of these newly-generated storms was determined by means of IR imagery from SMS-1. A total of 17 major dust occurrences were identified during the period June to September; 9 of these occurred during July. Most major dust storms occurred in a relatively localized region west of the Ahaggar mountains. By means of compositing methods, we found that all the major dust episodes occurred when a surface cyclone was present along the ITF, south of the dominant dust source region. This cyclone had to be sufficiently strong to generate geostrophic winds of at least about 17 knots (8.5 m/sec) over the source region.

Two types of flow patterns were observed in the 850-700 mb layer during dust episodes. One type is characterized by an anticyclonic flow pattern while the other is characterized by a cyclonic pattern with a 700 mb wave trough in the vicinity of the dust plume. None of these two types appear to agree with the previous model of the 700 mb flow pattern described by Carlson and Prospero (1972) for the eastern Atlantic.

The two types of flow pattern at the 850 - 700 mb layer are associated with two different types of isallobaric patterns at the surface. The anticyclonic flow pattern aloft is associated with pressure rises over Northwestern Africa, implying an intensification of a surface anticyclone over the area and a strengthening of the wind over the dust source region. On the other hand, the type with the cyclonic flow pattern aloft is associated with large pressure falls in the vicinity of the ITCZ, south of the dust source region as well as pressure rises to the north. The falls imply an intensification of a cyclone in the region of large

pressure falls. In this case, the increase in the wind speed in the source region is due to the intensification of both the surface cyclone and the anticyclone to the north. There are indications that the intensification of the anticyclone to the north or northeast of the surface cyclone is related to decreases in surface temperatures in the same area.

In summary, the occurrence of major dust clouds over the western Sahara is associated with several characteristic features of the large scale synoptic conditions, including the isallobaric pattern as well as the flow patterns at the 850-700 mb layer and the surface. A necessary ingredient for the occurrence of dust appears to be the existence of a well developed and intense surface cyclone along the ITF south of the dust source region. These three features are incorporated in three synoptic models for dust generation. The models are: the general model (GM), the model without a trough (NTM) and the model with a trough (TM). Conditions resembling those in the TM appear to be the ones most frequently observed during dust episodes in GATE.

Two other factors are related to the occurrence of large-scale dust storms: the pressure gradient between two selected points (a point 10 degrees to the north of the cyclone and the cyclone center itself) and the longitudinal location of the cyclone center relative to the dust source region. Our studies suggest that these two factors can be used to predict the occurrence of the dust clouds with a high degree of accuracy.

Finally, it should be noted that dust event statistics for the year 1974 might not be representative of normal meteorological conditions in North Africa a large portion of which was experiencing a drought which had begun in 1968 (Lamb, 1982). The drought was especially severe in the early 1970's. Large scale deflation increased sharply as a consequence of the drought and associated meteorological conditions (Middleton, 1985). Dust concentrations in the western Atlantic increased by a factor of three over values measured before the drought (Prospero and Nees, 1977, 1986).

Although the data presented here may not be representative of normal conditions, they do demonstrate that dust storm genesis in the western Sahara appears to occur under relatively well-defined meteorological conditions.

Acknowledgement

We acknowledge helpful discussions with D. Martin. This work was supported by Army Research Office Contract No. DAAG29-83-K0082.

REFERENCES

- Avila, L., 1984: Dust storm events over Asia and the mechanism which pumps dust into the atmosphere. M.S. Thesis, University of Miami, Coral Gables, FL., 74 pp.
- Carder, K.L., R.G. Steward, P.R. Betzer, D.L. Johnson and J.M. Prospero, 1986: Dynamics and composition of particles from an aeolian input event to the Sargasso Sea. *J. Geophys. Res.*, 91, 1055-1066.
- Carlson, T.N., J.M. Prospero, 1972: The large scale movement of Saharan air outbreaks over the northern equatorial Atlantic. *J. Appl. Meteor.*, 11, 283-287.
- Chen, L., and R.A. Duce, 1983: The sources of sulfate, vanadium and mineral matter in aerosol particles over Bermuda. *Atmos. Environ.* 17, 2055-2064.
- Delany, A.C., A.C. Delany, D.W. Parkin, J.J. Griffin, E.D. Goldberg and B.E.F. Reimann, 1967: Airborne dust collected at Barbados. *Geochim. Cosmochim. Acta*, 31, 885-909.
- Dubief, J., 1953: Les vents de sable au Sahara Fracais. *Colloques Internationaux du CNRS*, 35, 45-70.
- Dubief, J., 1959: Le climat du Sahara, Part I. *Universite D'Alger Memoire*, Alger, 312 pp.
- Dubief, J., 1979: Review of the North African climate with particular emphasis on the production of eolian dust in the Sahel zone and in the Sahara. In *Saharan Dust*, SCOPE Report 14, C. Morales, Ed., John Wiley and Sons, N.Y., 27-48.
- Fernandez-Partagas, J., D.M. Helgren and J.M. Prospero, 1986: Threshold wind velocities for raising dust in the western Sahara. *J. Clim. Appl. Meteorol.*, submitted.
- Gates, E.S., 1965: *Meteorology and Climatology for Sixth Form and Beyond*. George G. Harrap and Co., Ltd., London-Toronto-Wellington-Sidney, 225 pp.
- Gillette, D.A., 1979: Environmental factors affecting dust emission by wind erosion. In *Saharan Dust*, SCOPE Report 14, C. Morales, Ed., John Wiley and Sons, N.,Y., 71-91.
- Jaenicke, R., 1979: Monitoring and critical reveiw of the estimated source strength of mineral dust from the Sahara. In *Saharan Dust*, SCOPE Paper 14, C. Morales, Ed., John Wiley and Sons, N.Y., 233-242.
- Jaenicke, R., and L. Schutz, 1978: A comprehensive study of physical and chemical properties of the surface aerosols in the Cape Verde Island region. *J. Geophys. Res.*, 83, 3585-3599.

- Kalu, A.E., 1979: The African dust plume: Its characteristics and propagation across West Africa in winter. In Saharan Dust, SCOPE Report 14, C. Morales, Ed., John Wiley and Sons, N.Y., 95-118.
- Lamb, P.J., 1982: Persistence of Subsaharan drought. *Nature*, 299: 46-48.
- Lee, I.Y., 1983: Simulation of transport and removal processes of the Sahara dust. *J. Cli. Appl. Meteor.*, 22, 632-639.
- Merrill, J.T., R. Bleck, and L. Avila, 1985: Modeling atmospheric transport to the Marshall Islands. *J. Geophys. Res.*, 90, 12927-12936.
- Middleton, N.J., 1985: Effect of drought on dust production in the Sahel. *Nature*, 316, 431-434.
- Morales, C., 1979: The use of meteorological observations for studies of the mobilization, transport and deposition of Saharan soil dust. In Saharan Dust, SCOPE Report 14, C. Morales, Ed., John Wiley and Sons, N.Y., 119-129.
- Prospero, J.M., 1979: Mineral and sea-salt aerosol concentrations in various ocean regions. *J. Geophys. Res.*, 84, 725-731.
- Prospero, J.M., 1981a: Arid regions as sources of mineral aerosols in the marine atmosphere. In Desert Dust: Origin, Characteristics and Effect on Man, T.L. Pewe, Ed., Geological Society of America Special Paper 186, Boulder, Colorado, 71-86.
- Prospero, J.M., 1981b: Aeolian transport to the World Ocean. In The Oceanic Lithosphere, The Sea, Vol. 7, C. Emiliani, editor, Wiley Interscience, N.Y., 801-874.
- Prospero, J.M. and T.N. Carlson, 1972: Vertical and areal distribution of Saharan dust over the western equatorial North Atlantic Ocean. *J. Geophys. Res.*, 77, 5255-5265.
- Prospero, J.M. and R. Nees, 1977: Dust concentration in the atmosphere of the equatorial North Atlantic: Possible relationship to the Sahelian drought. *Science*, 196, 1196-1198.
- Prospero, J.M. and R. Nees, 1986: Mineral aerosols in the trade winds at Barbados: Impact of the North African drought and El Nino. *Nature*, in press.
- Prospero, J.M., D.L. Savoie, T.N. Carlson, and R.T. Nees, 1979: Monitoring Saharan aerosol transport by means of atmospheric turbidity measurements. In Saharan Dust, SCOPE Report 14, C. Morales, Ed., John Wiley and Sons, N.Y., 171-186.
- Prospero, J.M., R.A. Glaccum and R.T. Nees, 1981: Atmospheric transport of soil dust from Africa to South America. *Nature*, 289, 570-572.

Prospero, J.M., R.T. Nees and M. Uematsu, 1985: Deposition rate of dissolved and particulate aluminum derived from Saharan dust in precipitation at Miami, Florida. EOS, 66, 1309.

Schutz, L., R. Jaenicke and H. Pietrek, 1981: Saharan dust transport over the North Atlantic Ocean. In Desert Dust: Origin Characteristics and Effect on Man, T.L. Pewe, Ed., Geological Society of America Special Paper 186, Boulder, Colorado, 87-100.

Thompson, B.W., 1965: The Climate of Africa. Oxford University Press, Nairobi-New York.

Figure Captions

- Figure 1: Map of West Africa. Stippled areas are important highlands.
- Figure 2: Outlines of the nine major dust storms that occurred in July 1974 in the study region as determined from SMS-1 imagery.
- Figure 3: Climatological surface map for July (Thompson, 1965).
- Figure 4: Climatological 850 mb map for July (Thompson, 1965).
- Figure 5: Climatological 700 mb map for July (Thompson, 1965).
- Figure 6: Daily positions of all surface cyclone centers that occurred during the month of July 1974. The plus (+) signs mark the positions of cyclones associated with major dust events in July; the associated number is the date.
- Figure 7: Daily positions of all 700 mb troughs that occurred during the month of July 1974. The troughs marked with a wavy line are those associated with major dust events.
- Figure 8: Surface streamline map for July 2, 1974, with the outline of the dust event on this day.
- Figure 9: Surface streamline map for July 3, 1974, with the outline of the dust event on this day.
- Figure 10: Surface streamline map for July 8, 1974, with the outline of the dust event on this day.
- Figure 11: Surface streamline map for July 12, 1974, with the outline of the dust event on this day.
- Figure 12: Surface streamline map for July 21, 1974, with the outline of the dust event on this day.
- Figure 13: Surface streamline map for July 22, 1974, with the outline of the dust event on this day.
- Figure 14: Surface streamline map for July 23, 1974, with the outline of the dust event on this day.
- Figure 15: Surface streamline map for July 28, 1974, with the outline of the dust event on this day.
- Figure 16: Surface streamline map for July 29, 1974, with the outline of the dust event on this day.
- Figure 17: Dust storm plume positions relocated relative to the mean position of the cyclones.
- Figure 18: The composite plume for all nine major dust events of July 1974 and the associated composite large scale flow pattern.

- Figure 19: The composite dust plume for anticyclonic dust storm events (July 2, 3, 12, 28, 29) and the associated composite large scale flow pattern.
- Figure 20: The composite dust plume for cyclonic dust storm events (July 8, 21, 22, 23) and the associated composite large scale flow pattern.
- Figure 21: The composite dust plume and the associated isallobaric patterns.
- Figure 22: Isallobaric pattern for dust events occurring during anticyclonic flow conditions.
- Figure 23: Isallobaric pattern for dust events occurring during cyclonic flow conditions.
- Figure 24: Composite of 24 hour surface temperature changes for the region north and northeast of the surface cyclone for all dust event days in July.
- Figure 25: Temperature records (1200 GMT) for a) Marrakech and b) Ouarzazate.
- Figure 26: Schematic features for the General Model.
- Figure 27: Schematic features for the Trough Model.
- Figure 28: Schematic features for the Non Trough Model.
- Figure 29: 850-700 mb streamlines and 24-hr pressure changes for June 28, 1974, with the outline of the dust event on this day. The plus sign marks the cyclone center.
- Figure 30: 850-700 mb streamlines; 24-hr pressure changes and cyclone center for June 29, 1974, with the outline of the dust event on this day.
- Figure 31: 850-700 mb streamline; 24-hr pressure changes and cyclone center for June 30, 1974, with the outline of the dust event on this day.
- Figure 32: 850-700 mb streamlines, 24-hr pressure changes and cyclone center for August 2, 1974, with the outline of the dust event on this day.
- Figure 33: 850-700 mb streamlines, 24-hr pressure changes and cyclone center for August 8, 1974, with the outline of the dust event on this day.
- Figure 34: 850-700 mb streamlines, 24-hr pressure changes and cyclone center for August 9, 1974, with the outline of the dust event on this day.

- Figure 35: 850-700 mb streamlines, 24-hr pressure changes and cyclone center for August 25, 1974, with the outline of the dust event on this day.
- Figure 36: 850-700 mb streamlines, 24-hr pressure changes and cyclone center for September 3, 1974, with the outline of the dust event on this day.
- Figure 37: Top, the daily surface pressures at 30°N , 0° and at 20°N 0° . Bottom, the pressure difference between these points (left hand scale) and the east-west component of the geostrophic wind (right hand scale). Days on which dust events occurred are marked with a dashed line.
- Figure 38: Ordinate, the position of the cyclone center relative to the longitude of the major dust source region. Abscissa, the pressure difference between the cyclone and the region 10° to the north. Each point corresponds to a day in the study period. An "X" indicates a day on which a major dust event occurred.

Table 1. Ranked Value of Pressure Gradients in Relation to Dust Occurrence

Rank No.	Pres. Grad. (mb/10 ⁰ Lat)	Date (July 1974)	Cyclone Loc. (Lat, Long)	Dust Occurr.	Rank No.	Pres. Grad. (mb/10 ⁰ Lat)	Date (July 1974)	Cyclone Loc. (Lat, Long)	Dust Occurr.
1	11	21	21N, 9E	No	19	6	28	18N, 8E	No
2	10	21	19N, 7E	No	20	5	6	20N, 5W	No
3	10	21	23N, 3E	Yes	21	5	10	19N, 1E	No
4	9	11	20N, 0E	No	22	5	18	17N, 8W	No
5	9	22	22N, 2E	Yes	23	5	20	20N, 0	No
6	8	4	22N, 9W	No	24	5	28	20N, 3W	Yes
7	8	9	22N, 2E	No	25	4	14	21N, 3E	No
8	8	29	20N, 7W	Yes	26	4	18	22N, 2E	No
9	7	2	20N, 2W	Yes	27	4	19	22N, 2E	No
10	7	3	21N, 4W	Yes	28	4	20	20N, 8W	No
11	7	9	21N, 7W	No	29	4	27	20N, 0	No
12	7	14	21N, 9W	No	30	17	17	19N, 0	No
13	7	23	22N, 3E	Yes	31	26	26	21N, 1W	No
14	6	7	20N, 8W	No	32	31	31	23N, 0W	No
15	6	8	21N, 1W	Yes	33	13	13	20N, 7W	No
16	6	11	17N, 9E	No	34	19	19	18N, 8E	No
17	6	12	20N, 1W	Yes	35	15	15	17N, 3E	No
18	6	24	22N, 1W	No					

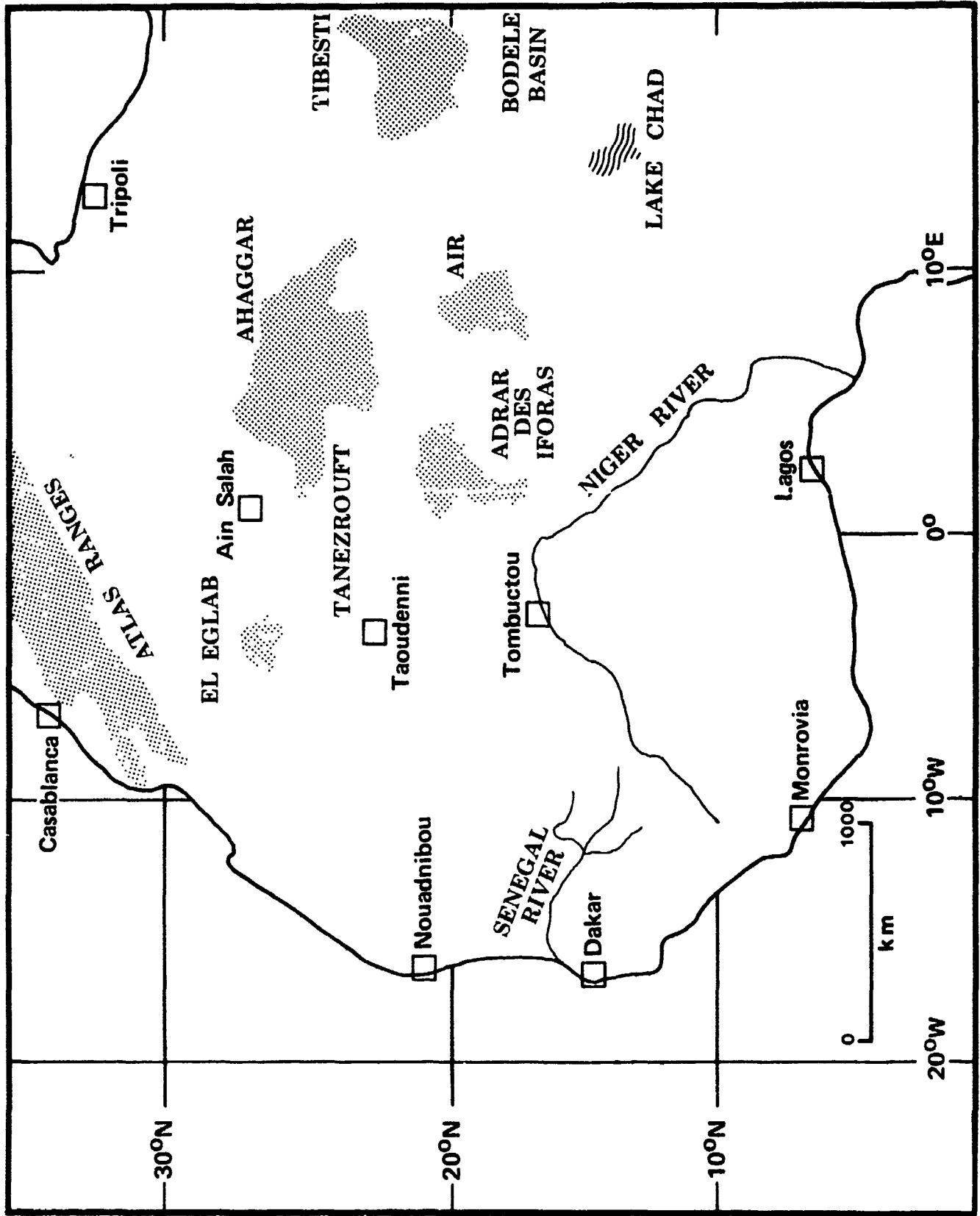


Figure 1

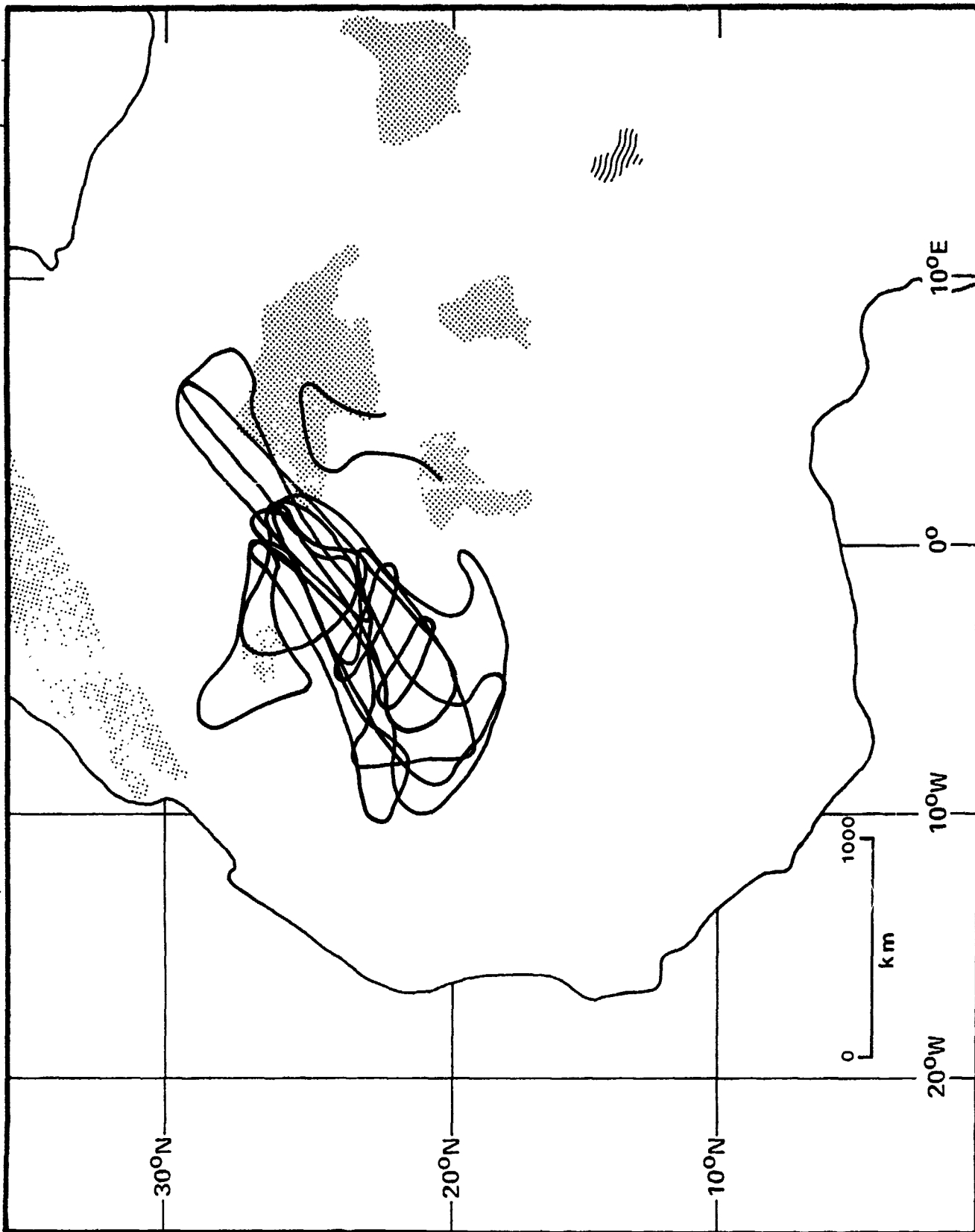


Figure 2

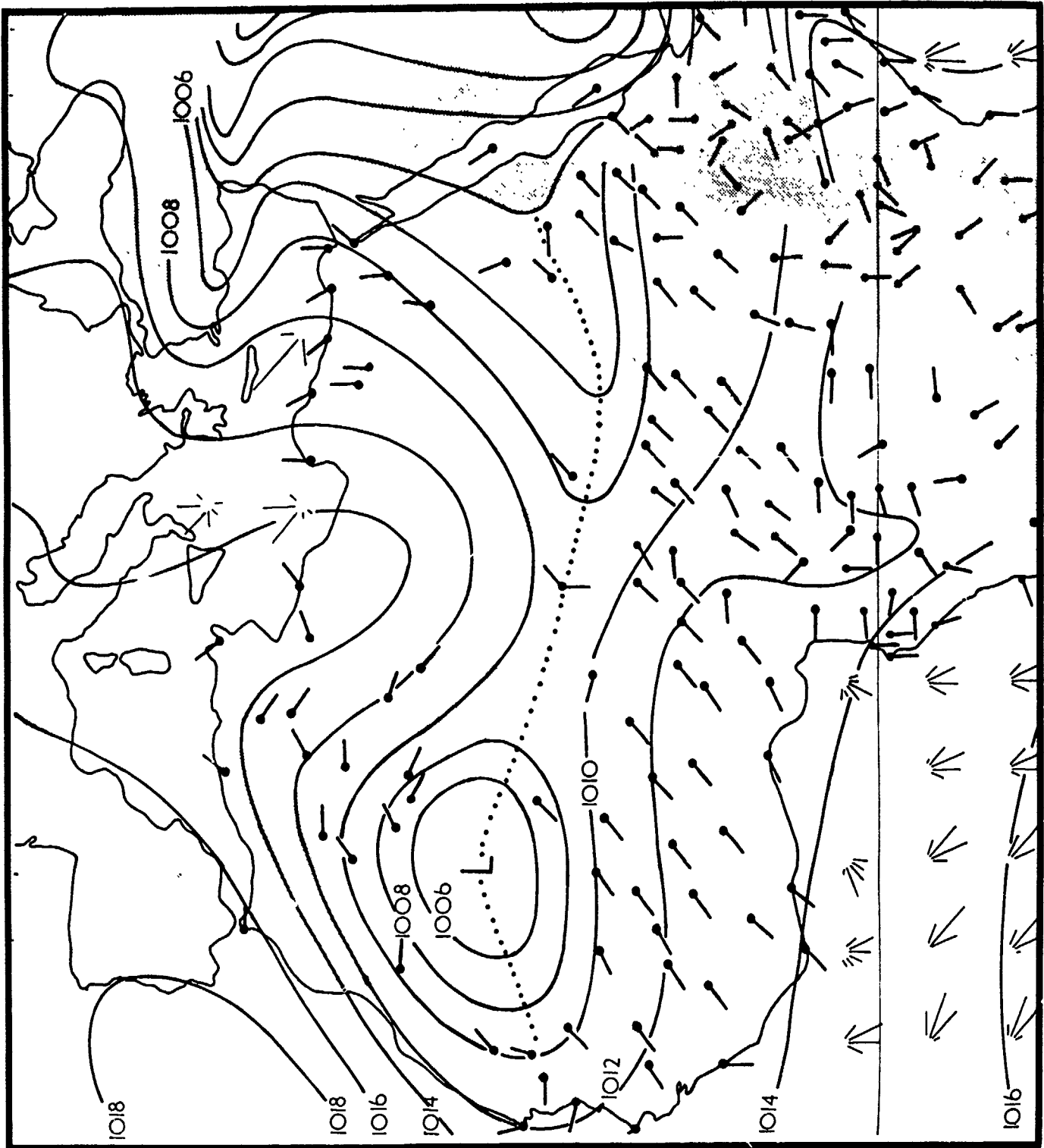


Figure 3

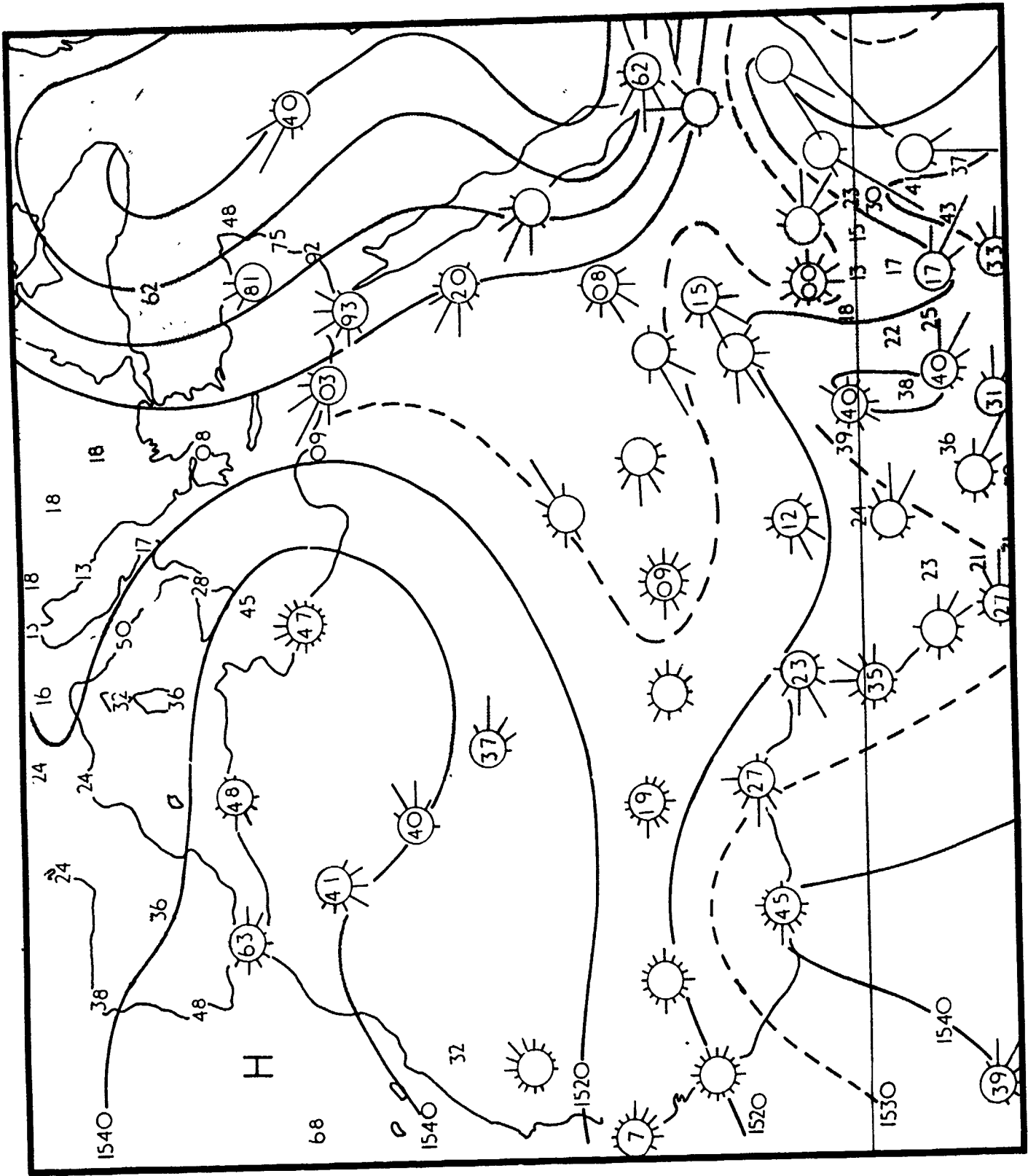


Figure 4

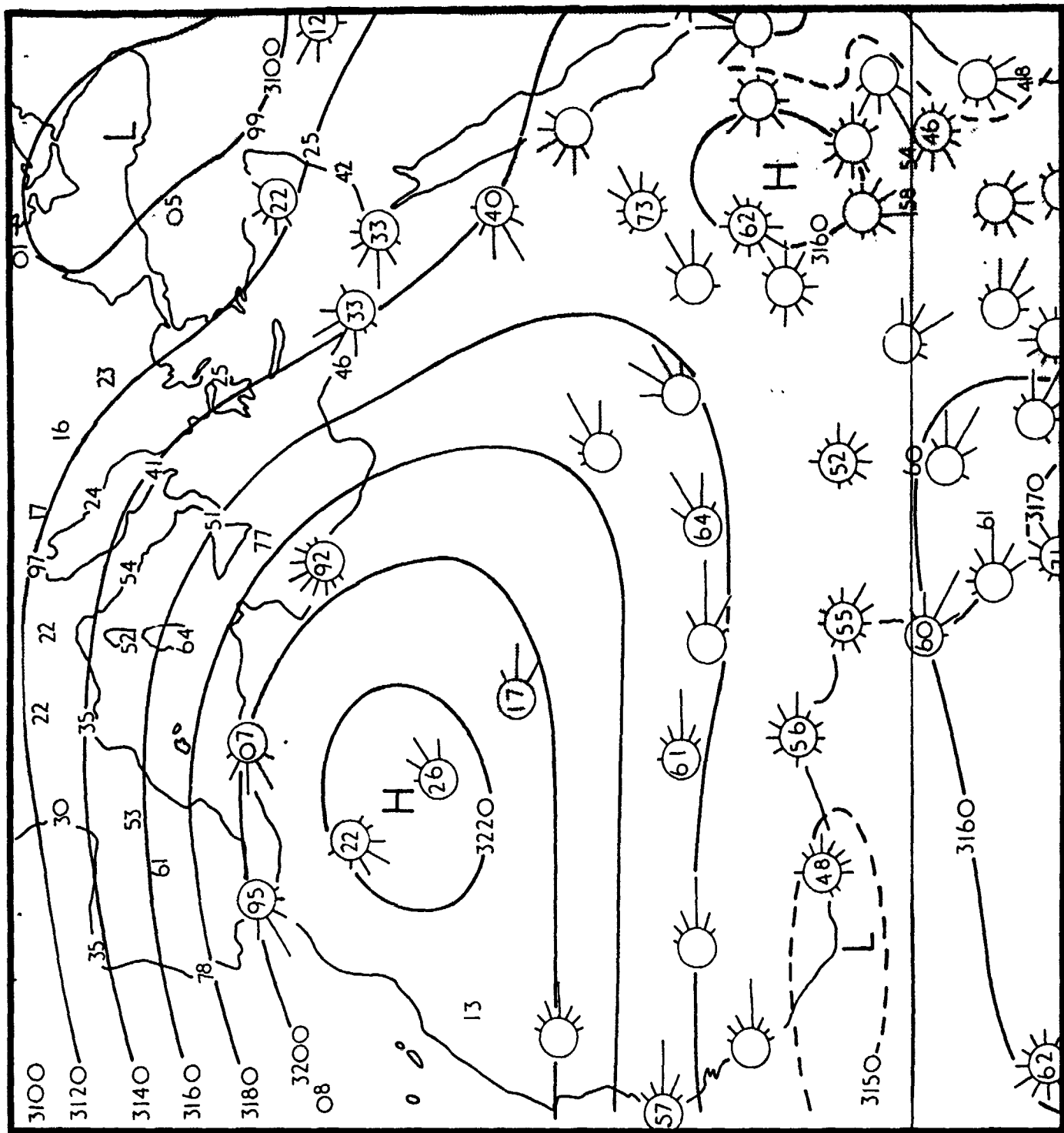


Figure 5

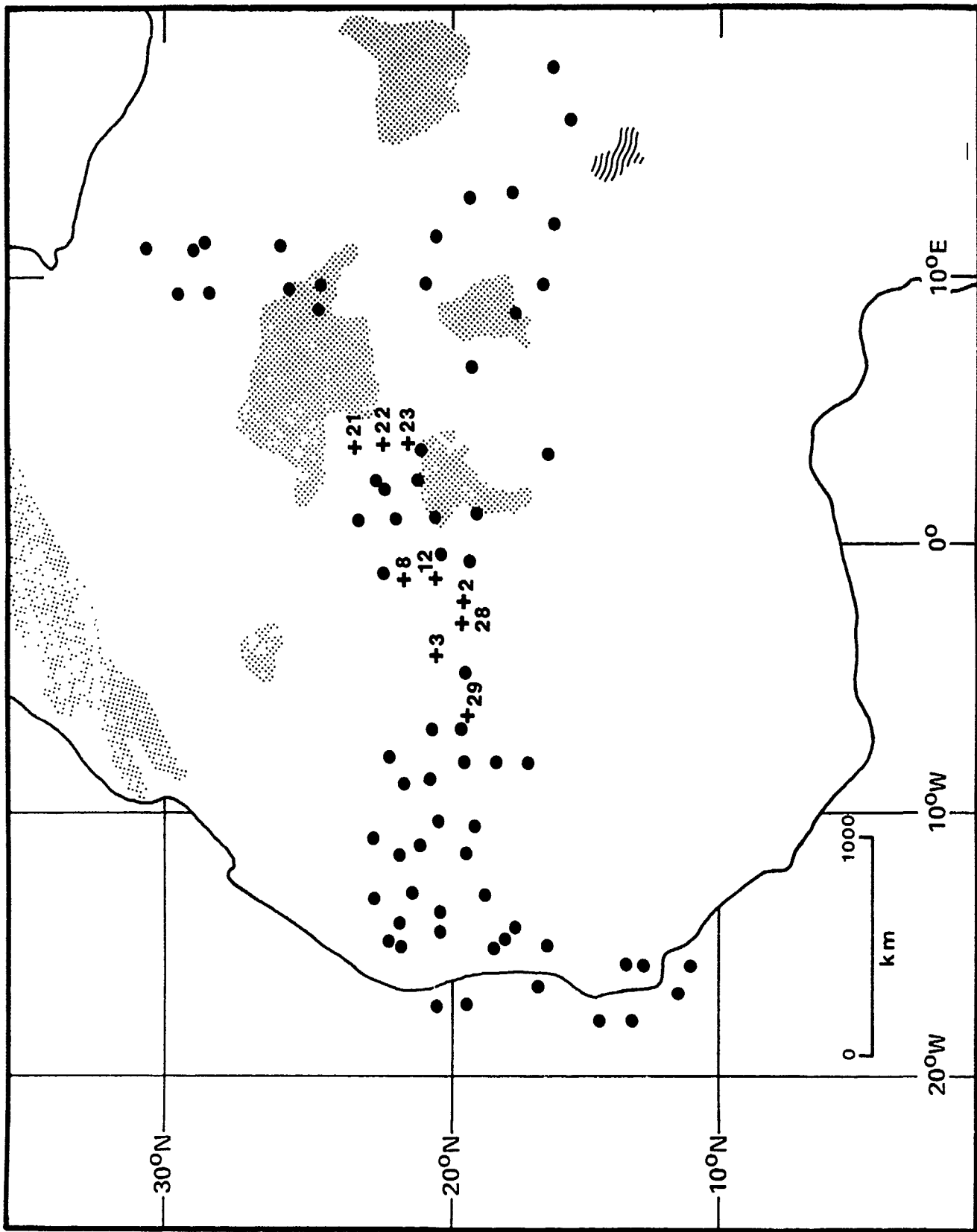


Figure 6

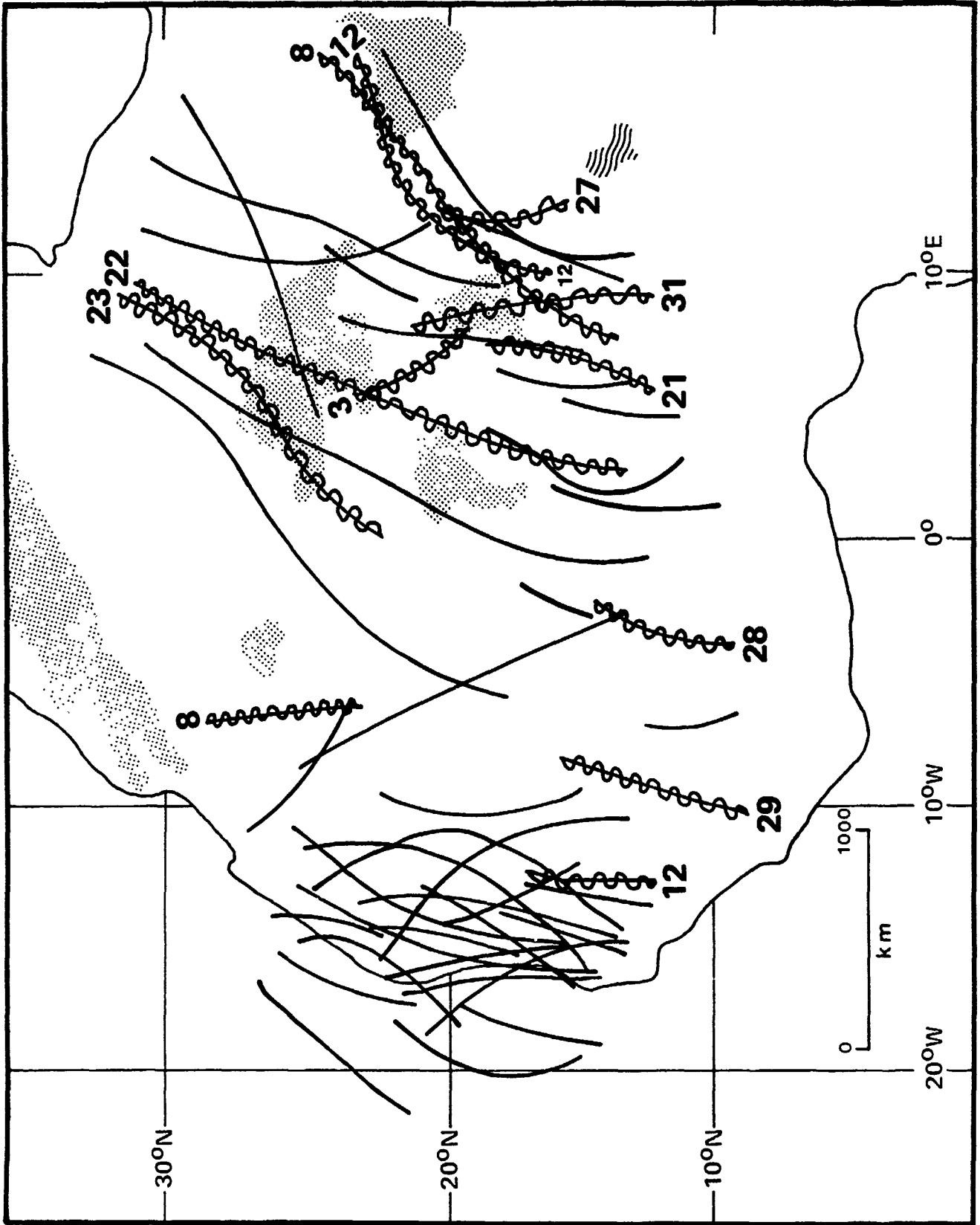


Figure 7

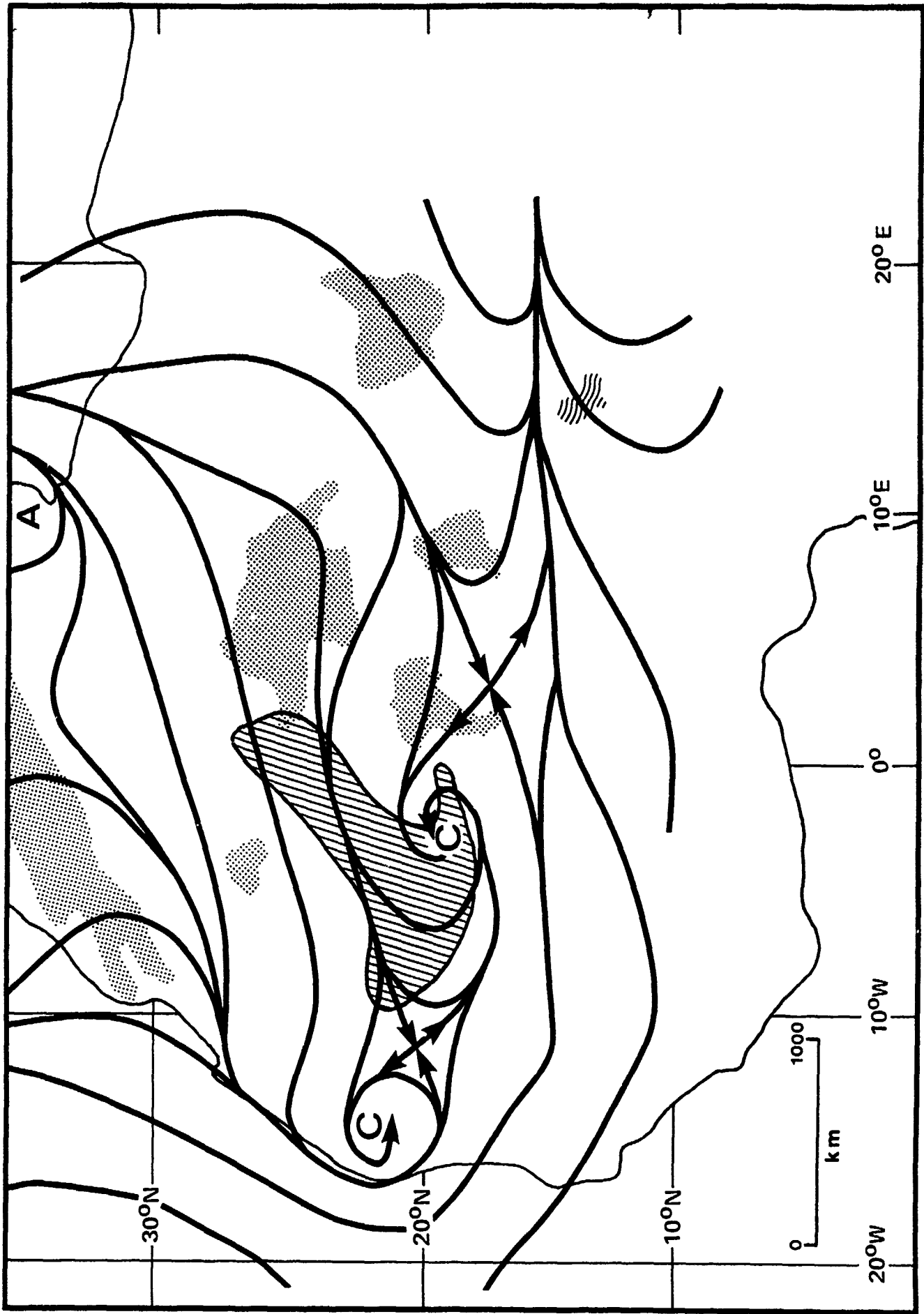


Figure 8

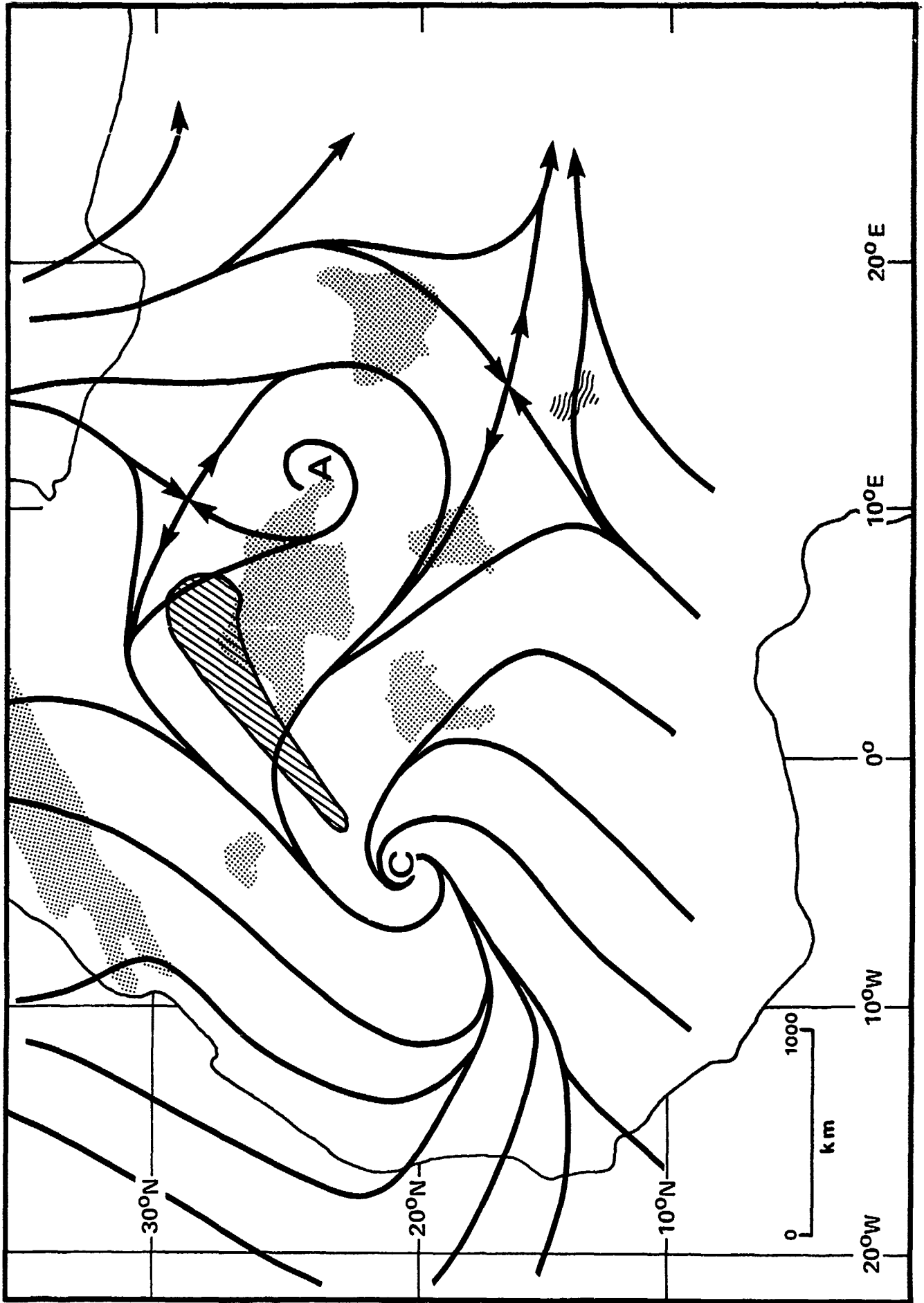


Figure 9

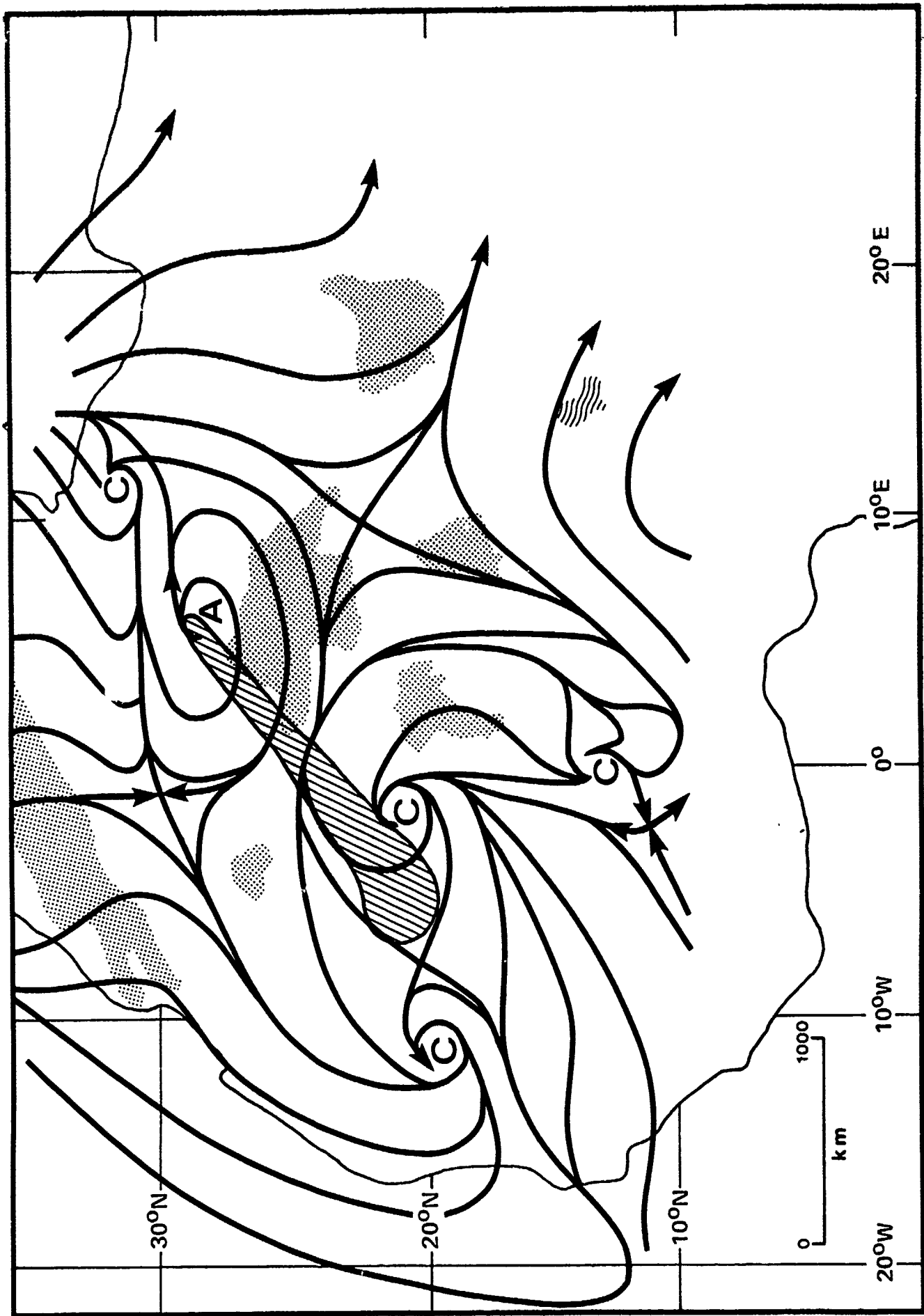


Figure 10



Figure 11

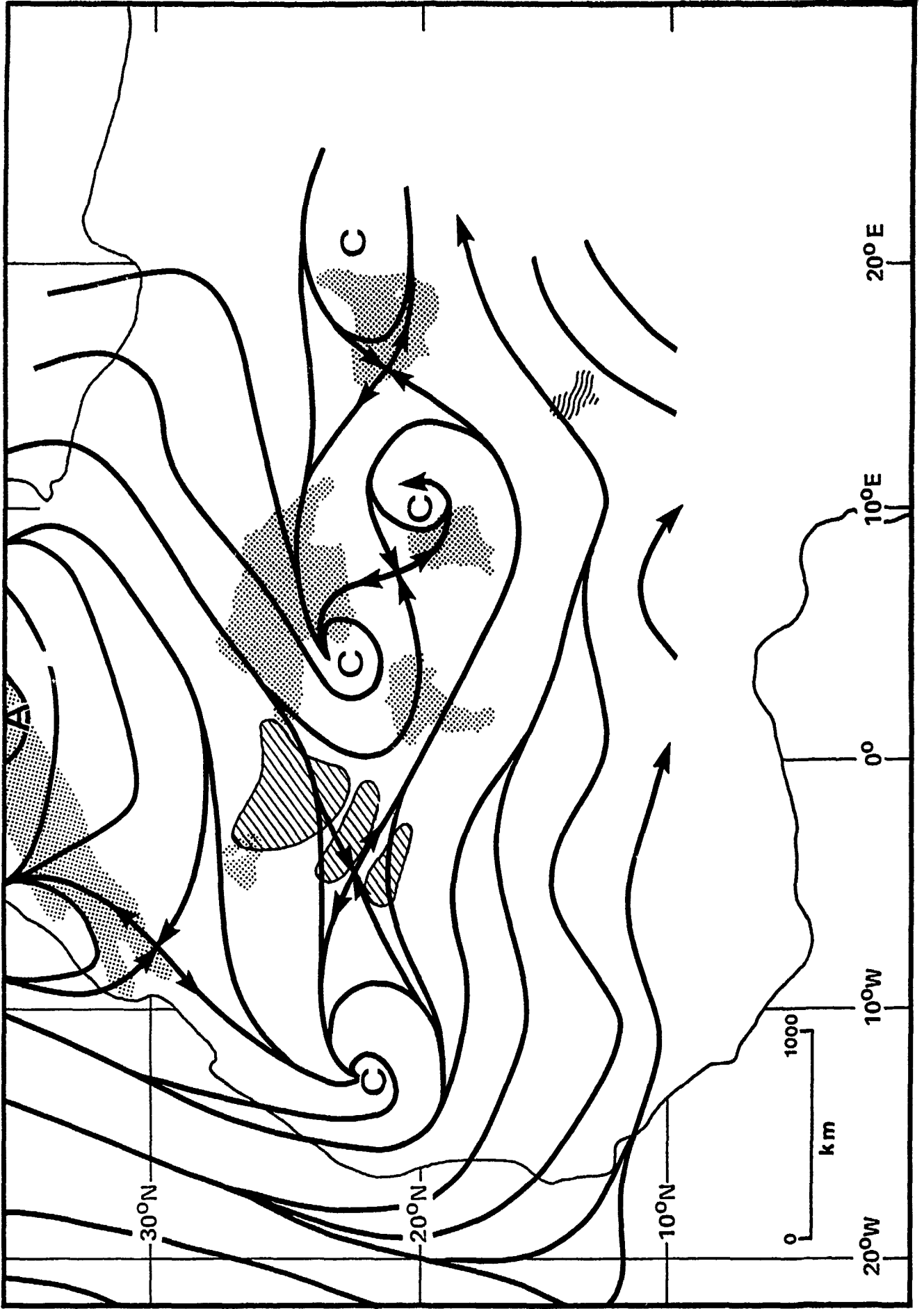


Figure 12

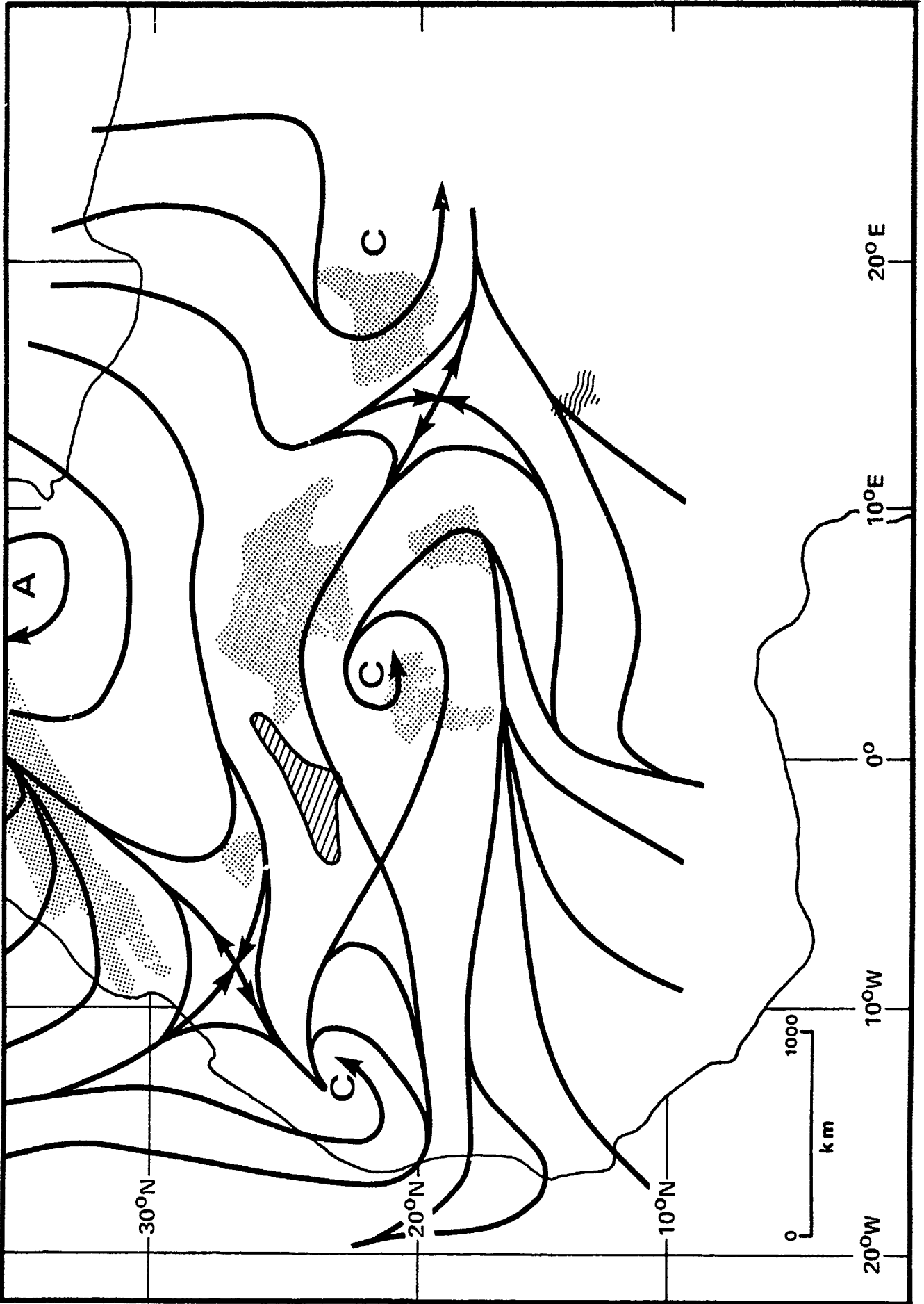


Figure 13

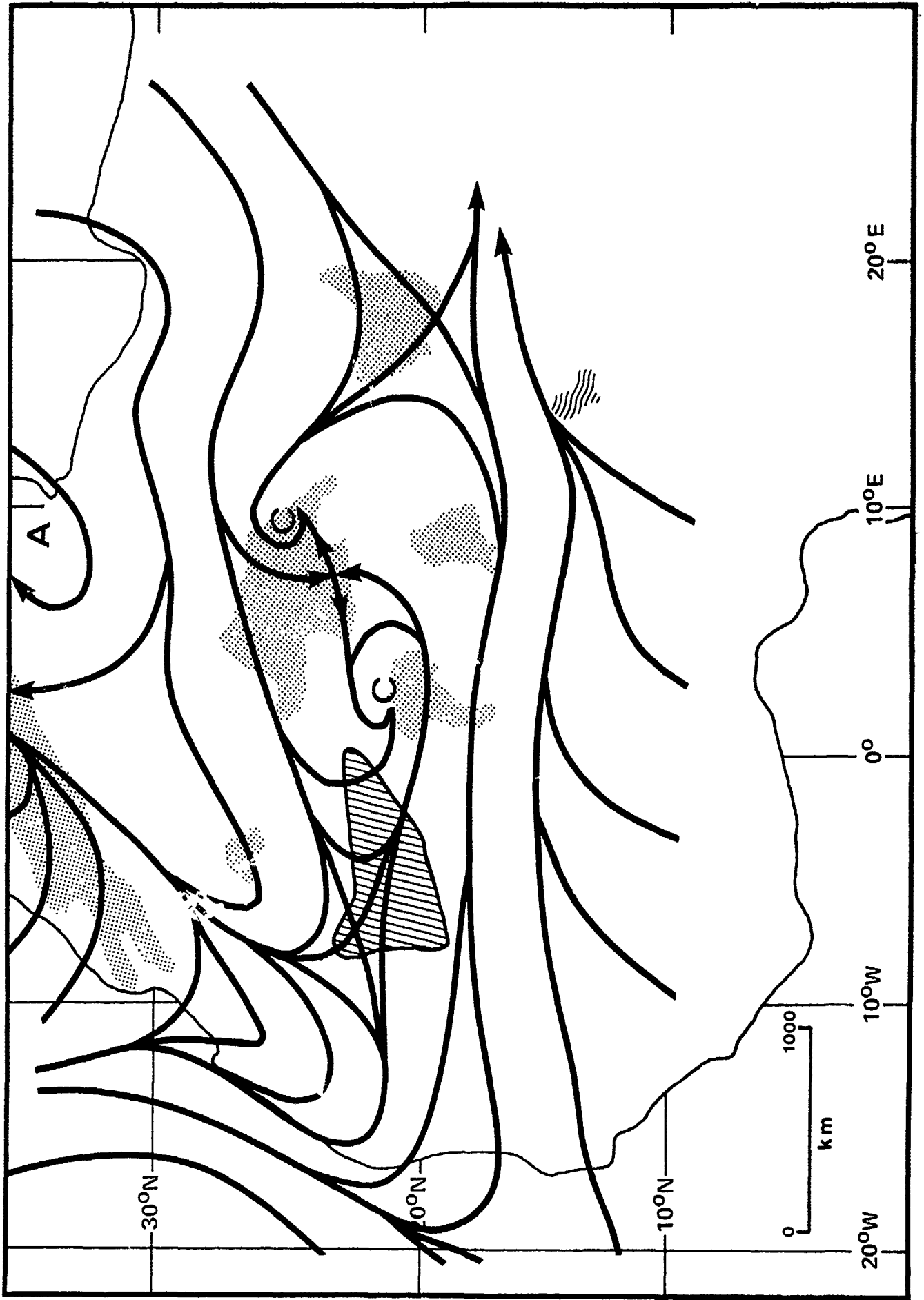


Figure 14

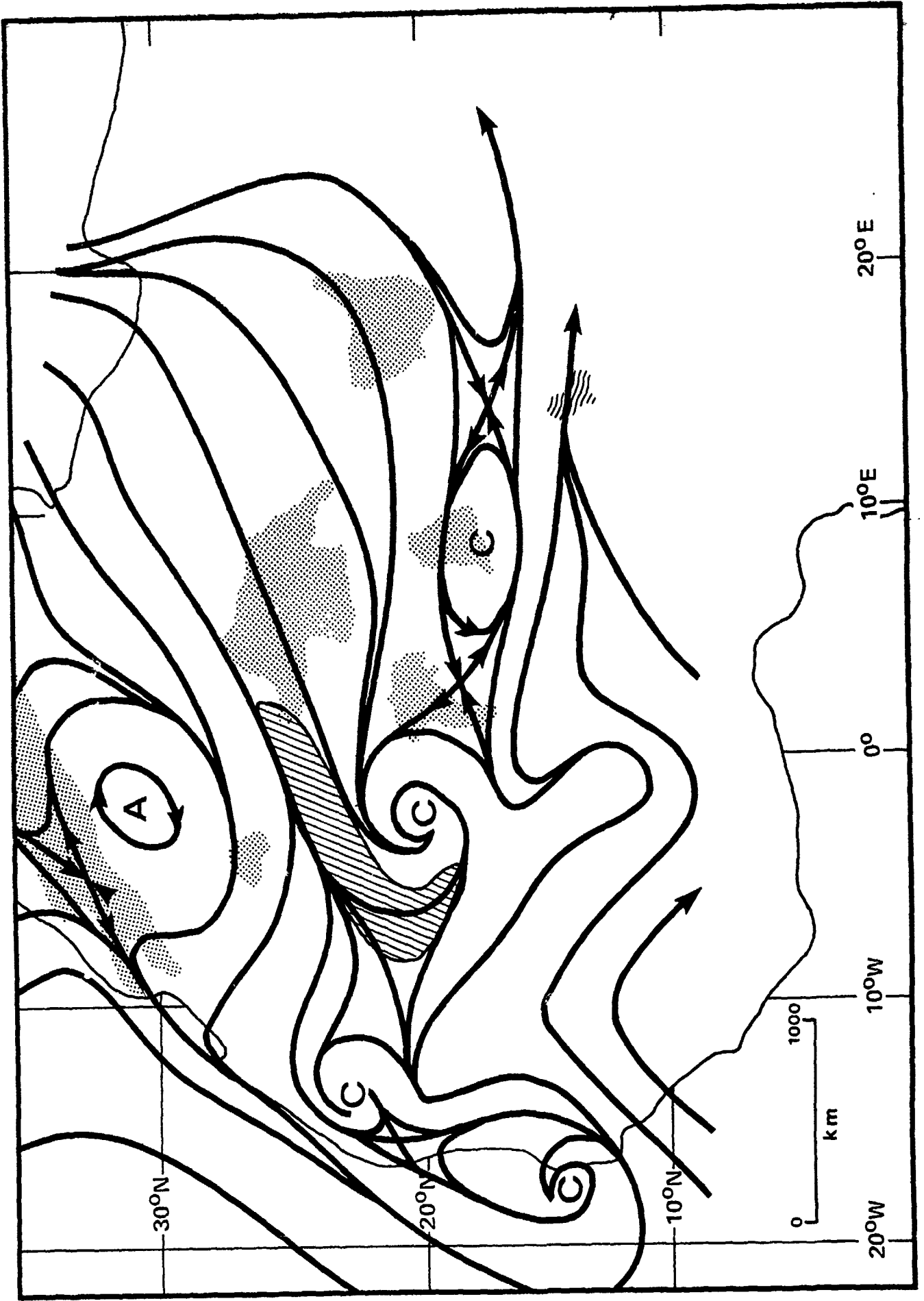


Figure 15

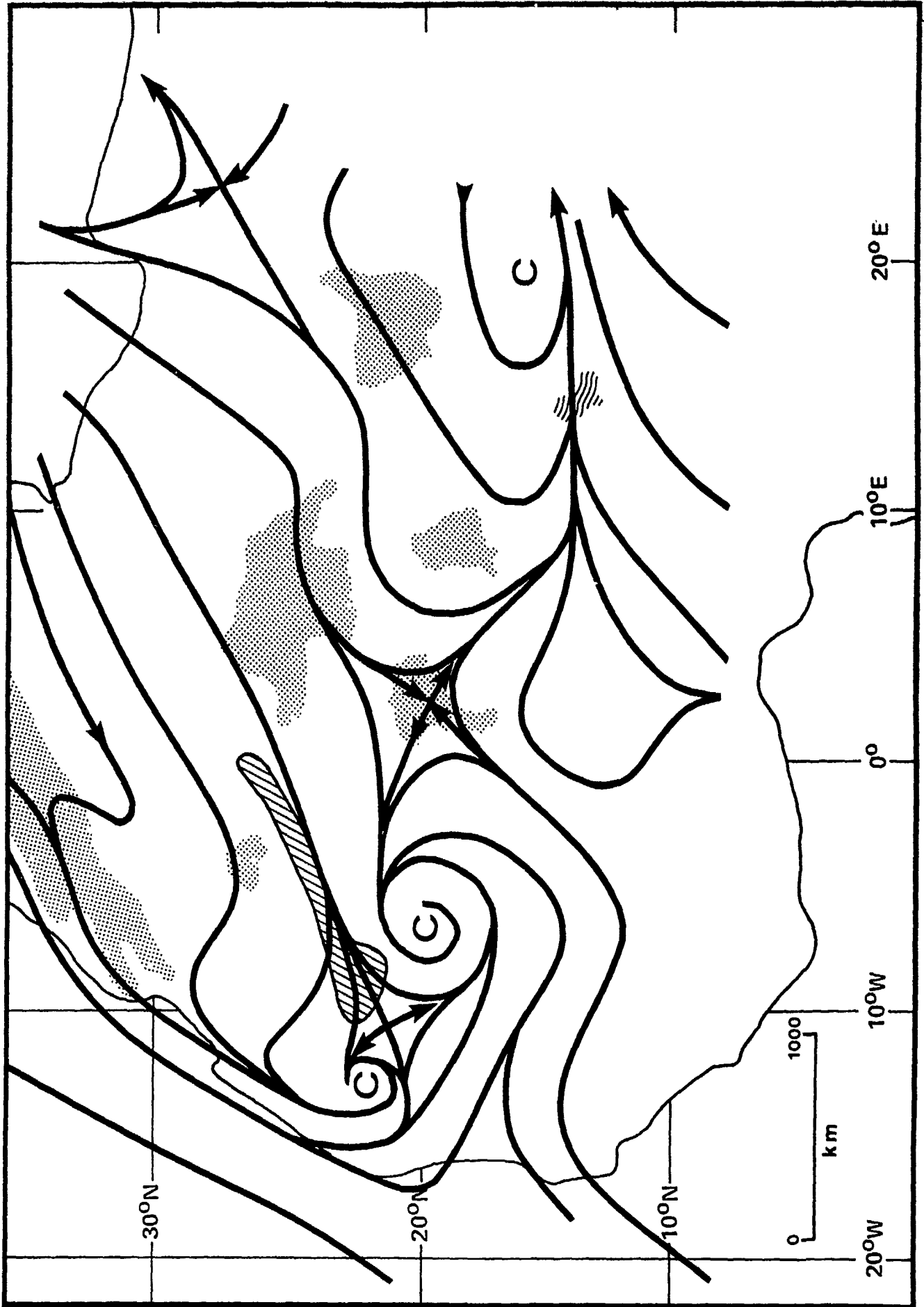


Figure 16

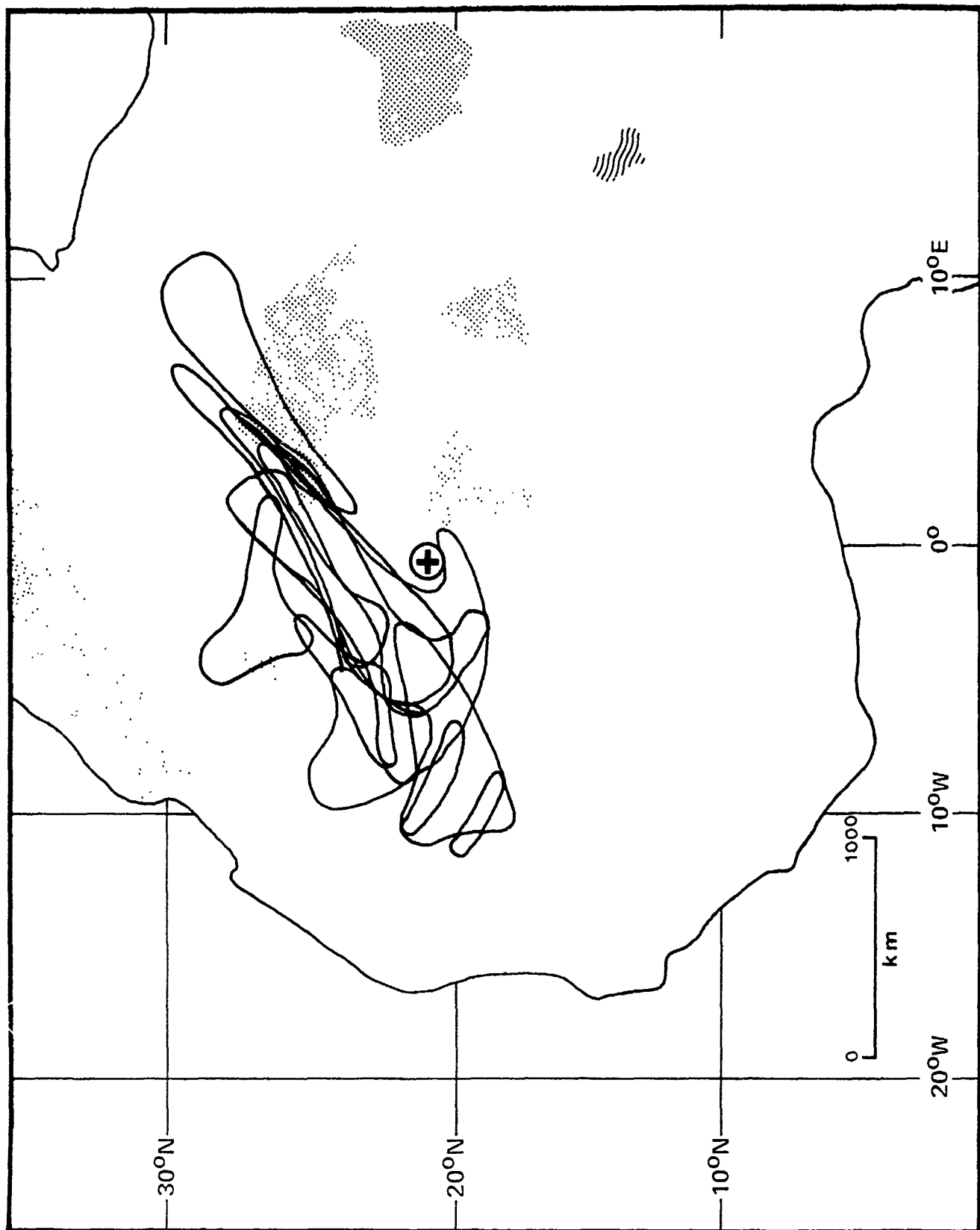


Figure 17

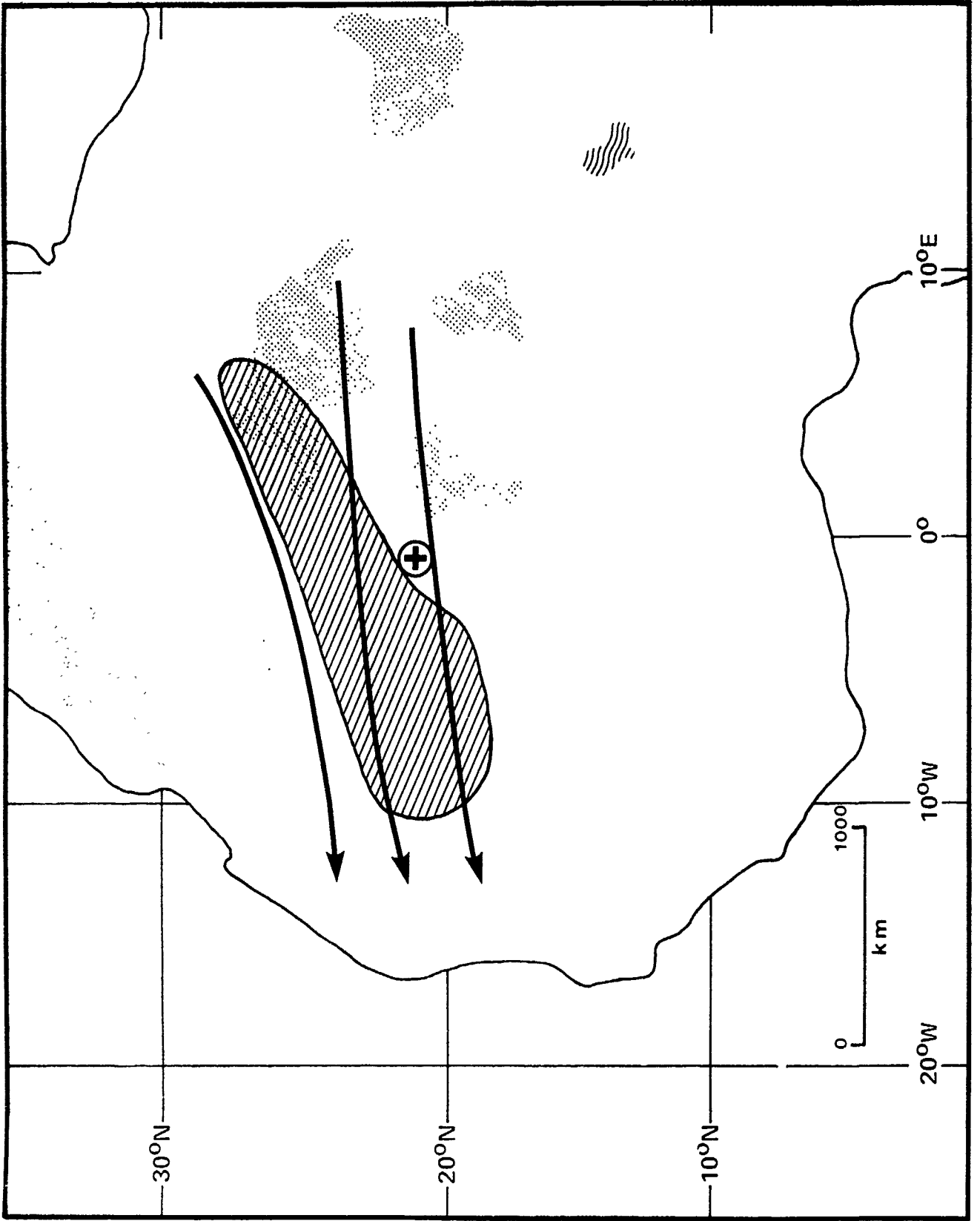


Figure 18

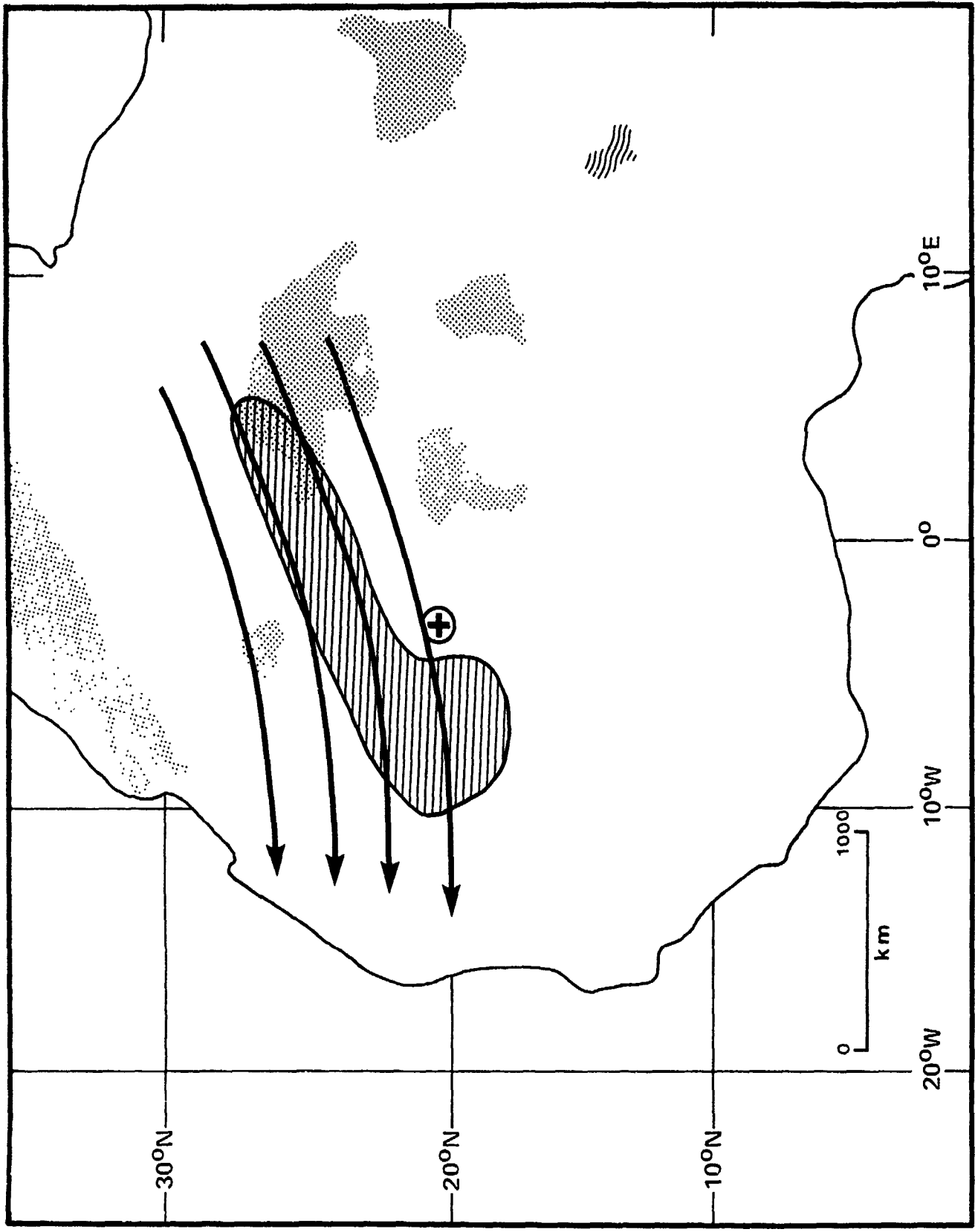


Figure 19

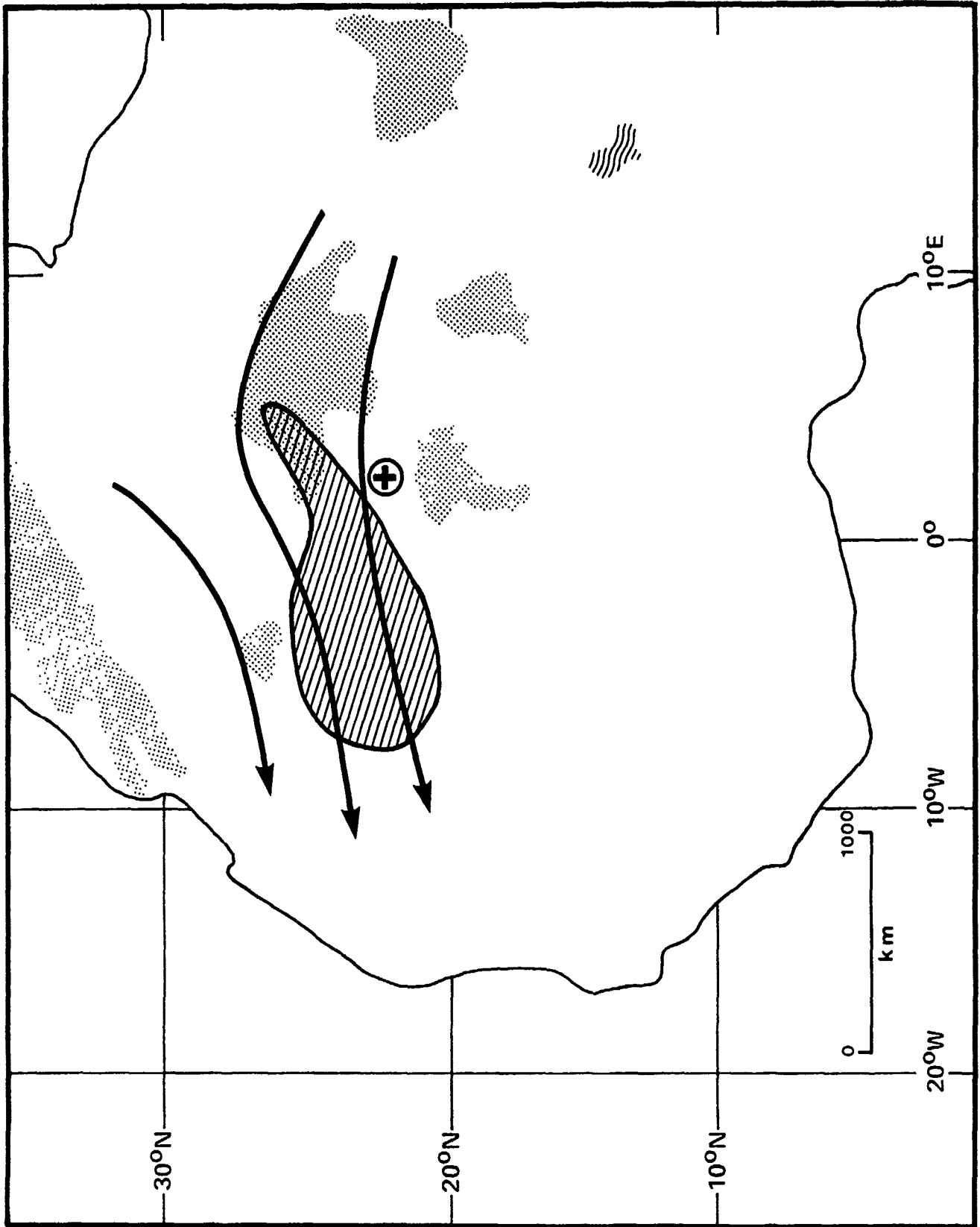


Figure 20

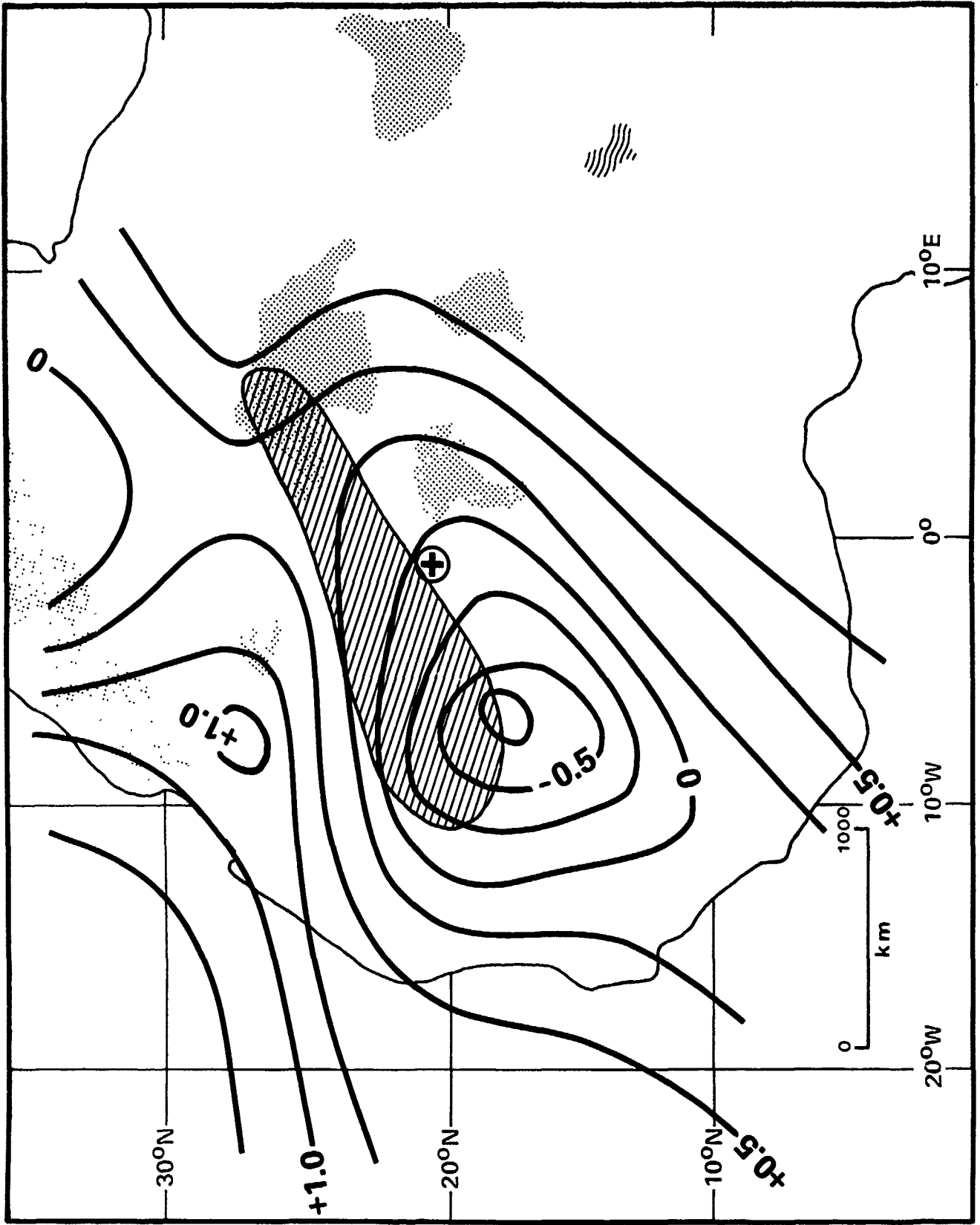


Figure 21

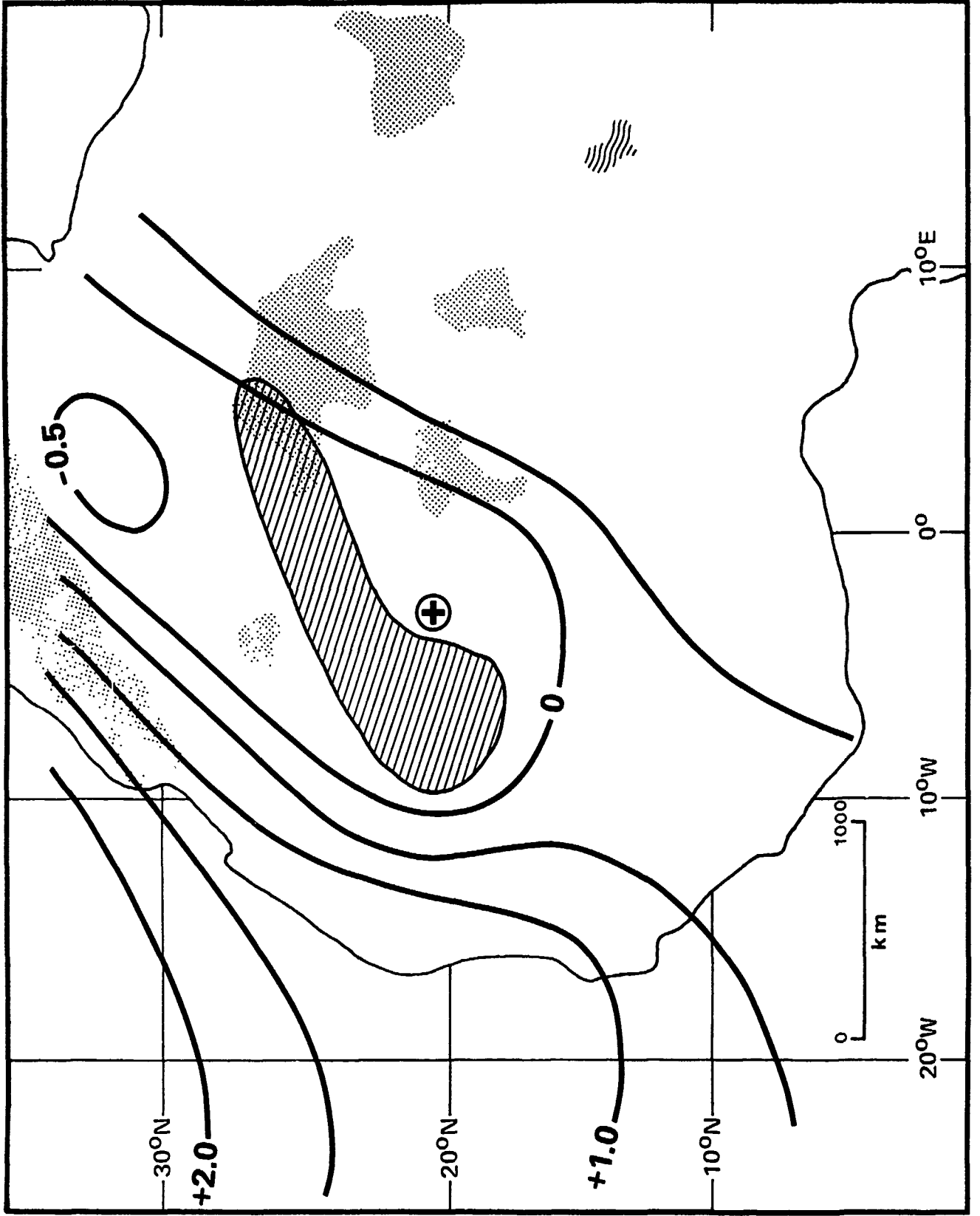


Figure 22

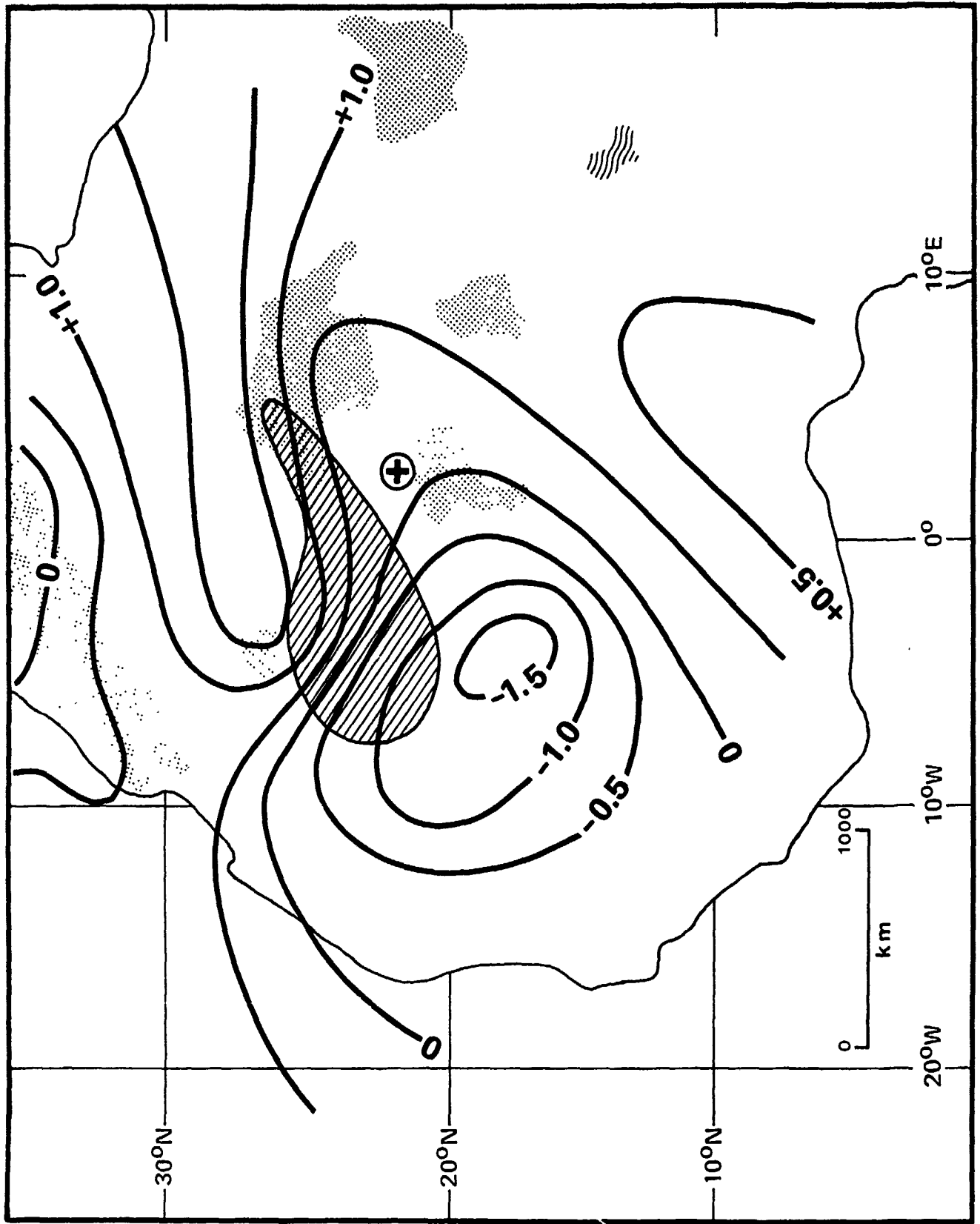


Figure 23

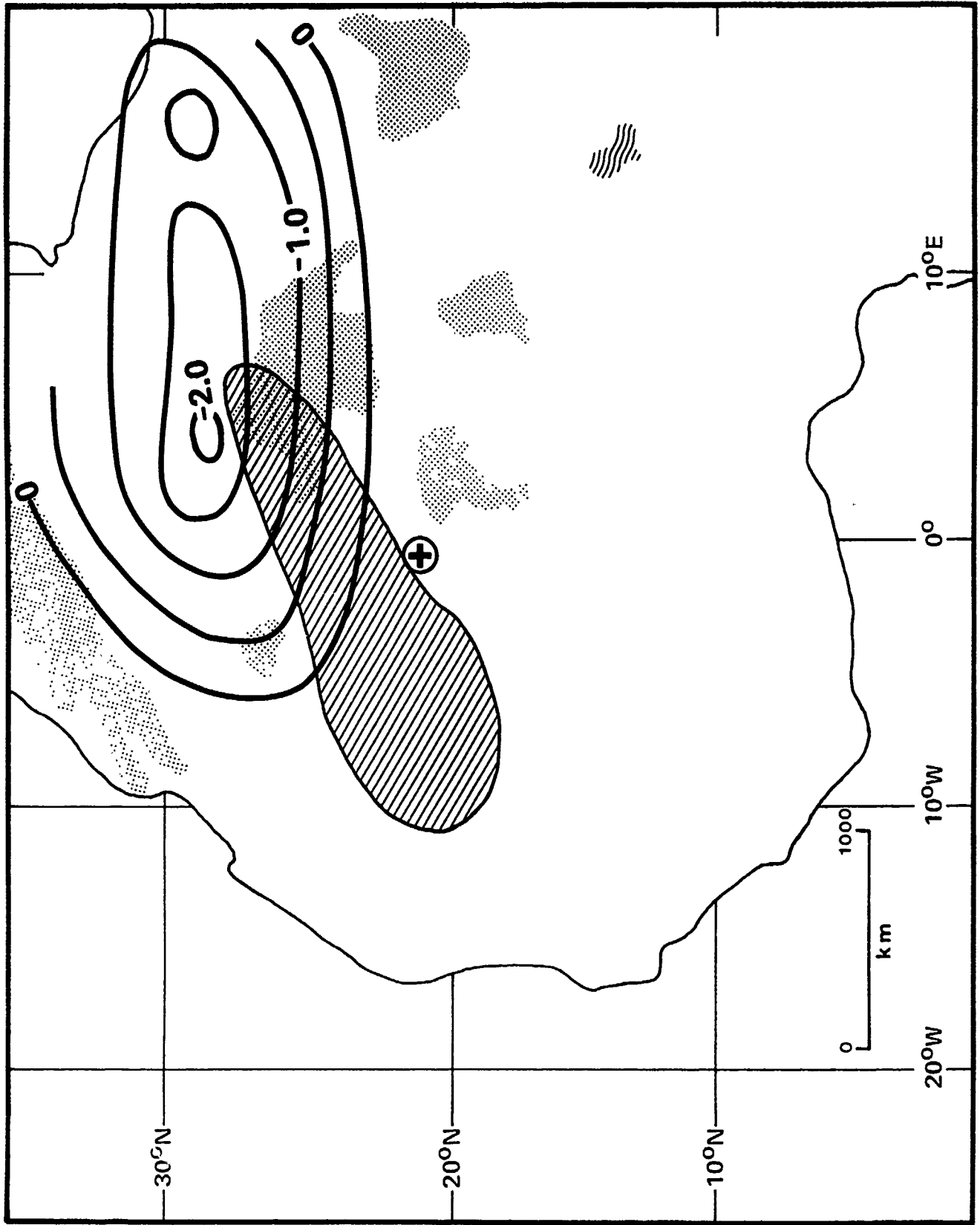


Figure 24

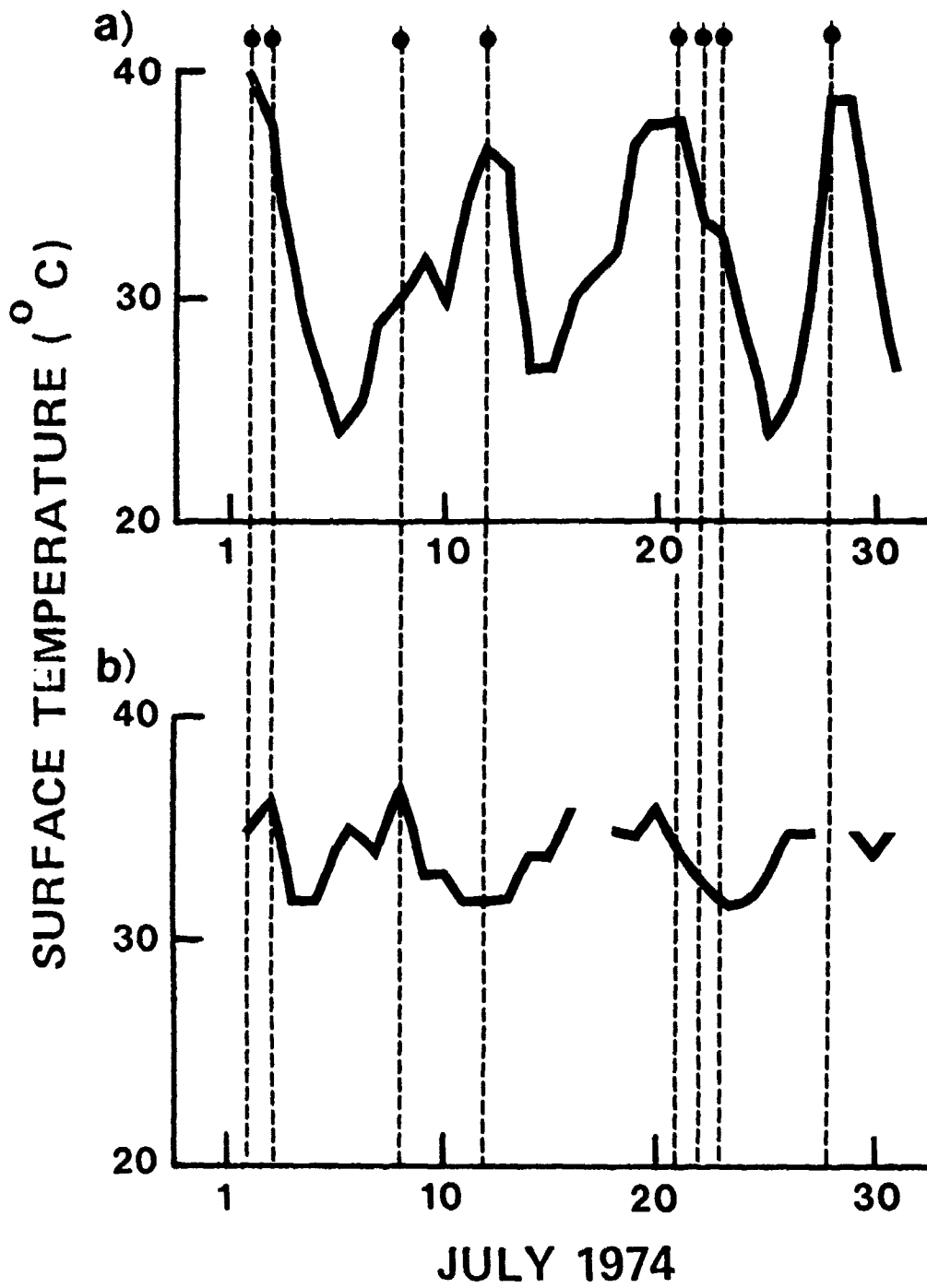


Figure 25

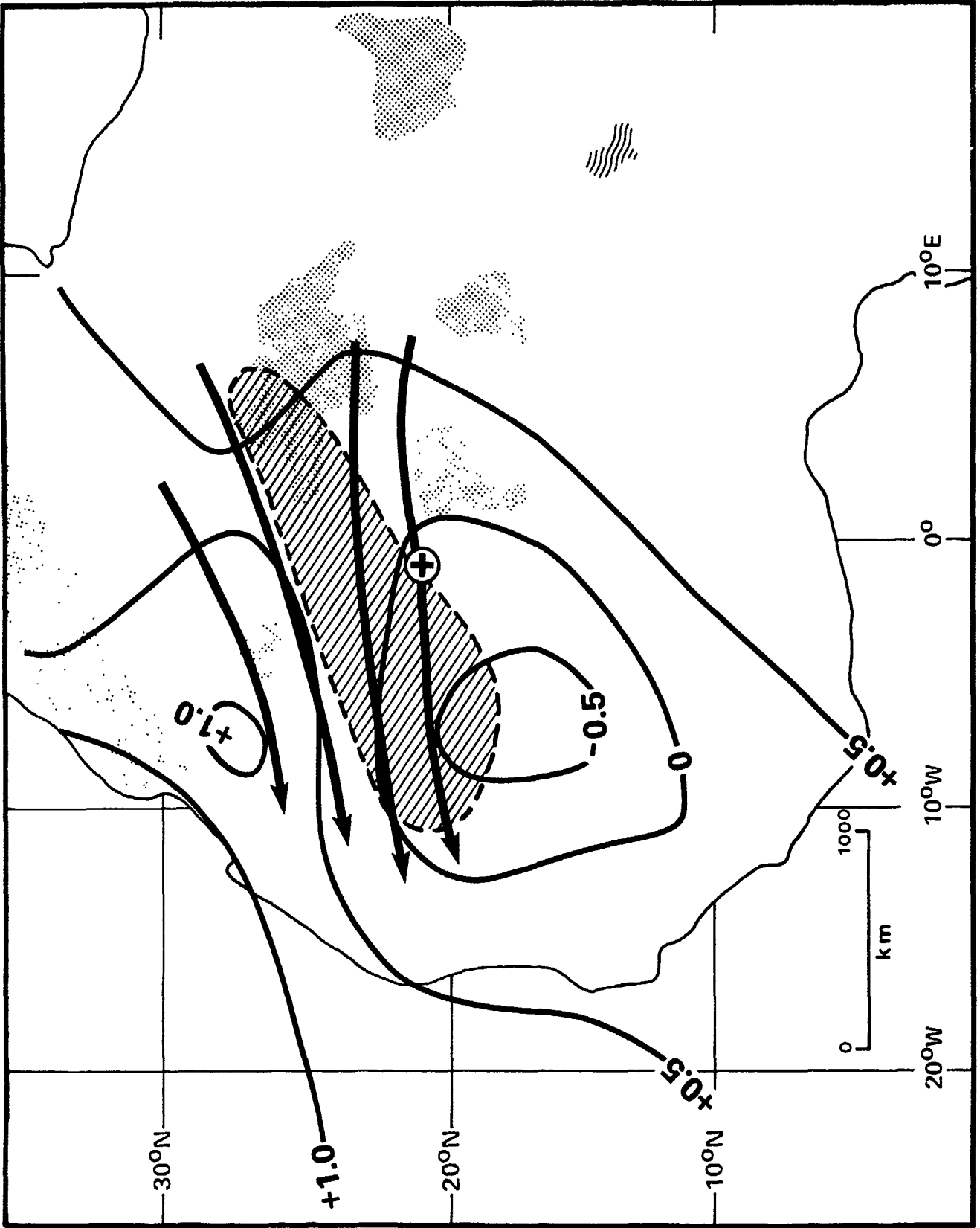


Figure 26

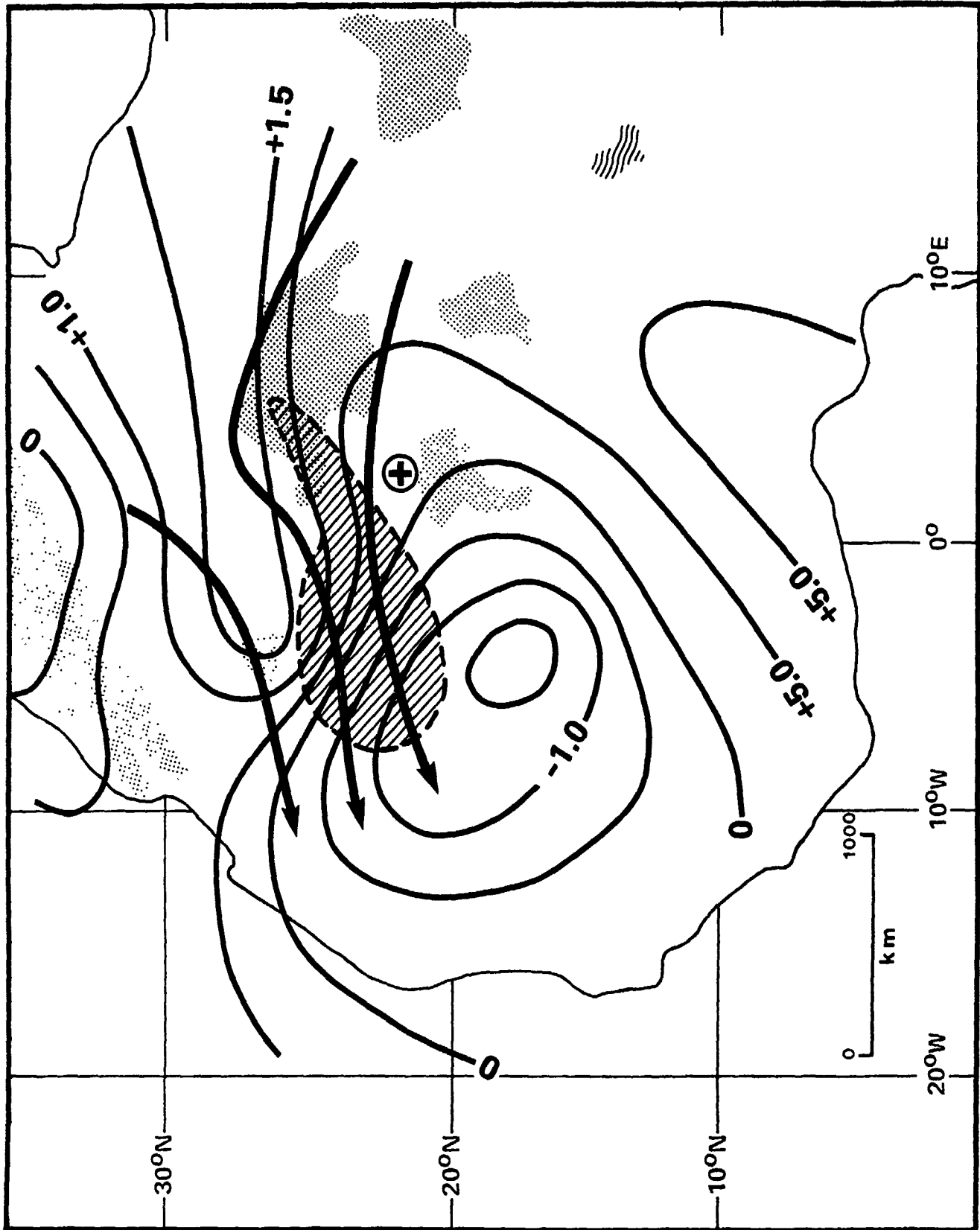


Figure 27

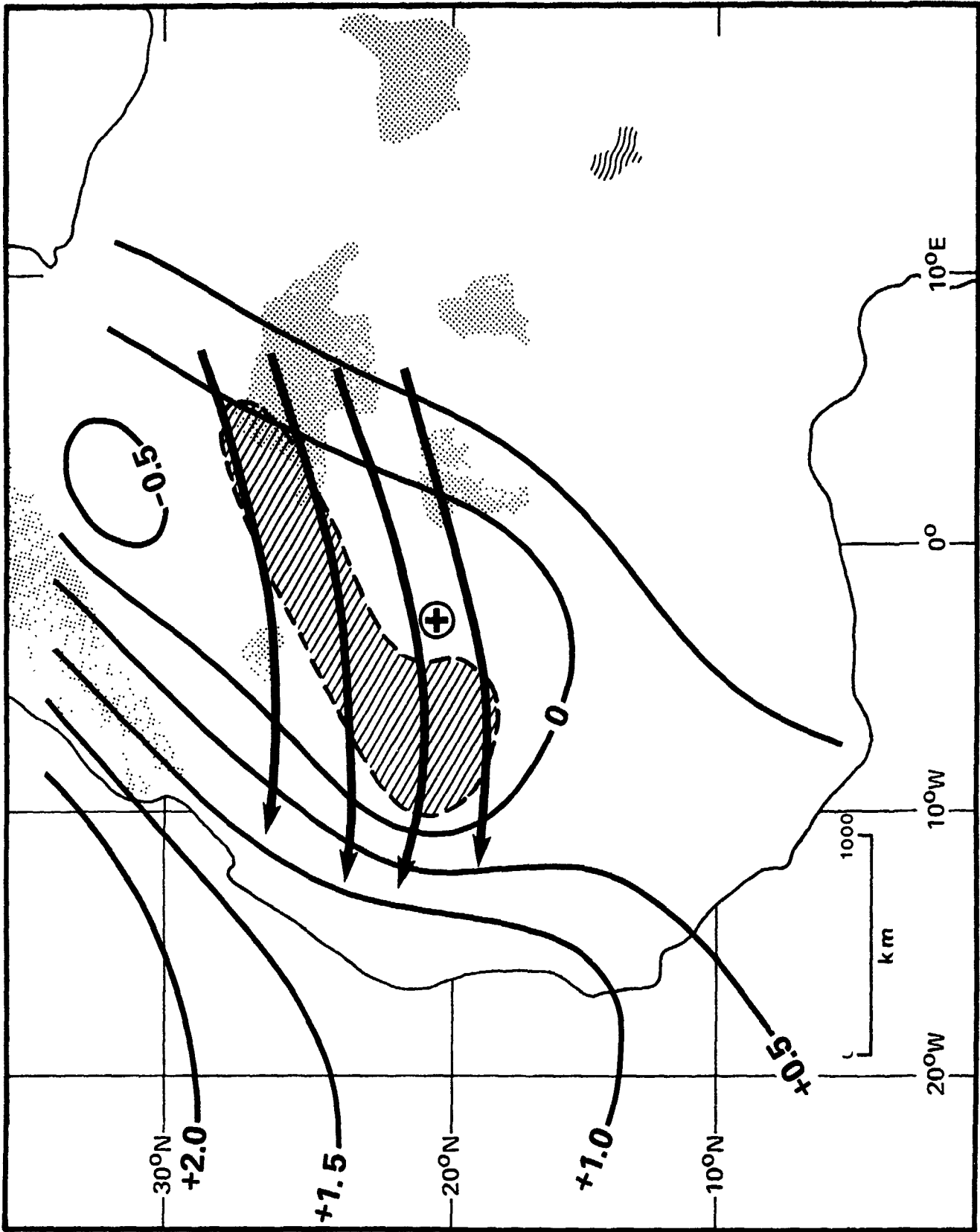


Figure 28

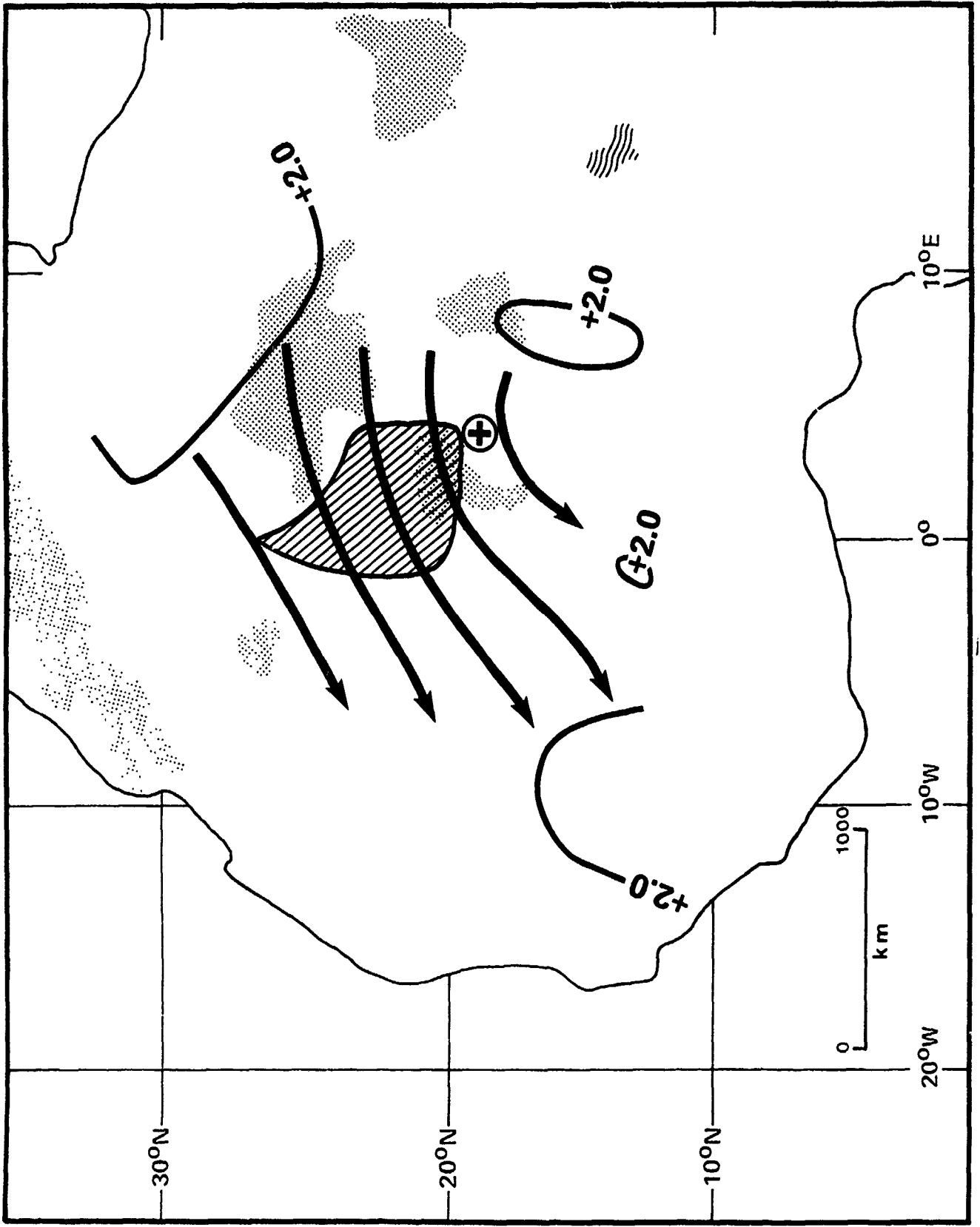


Figure 29

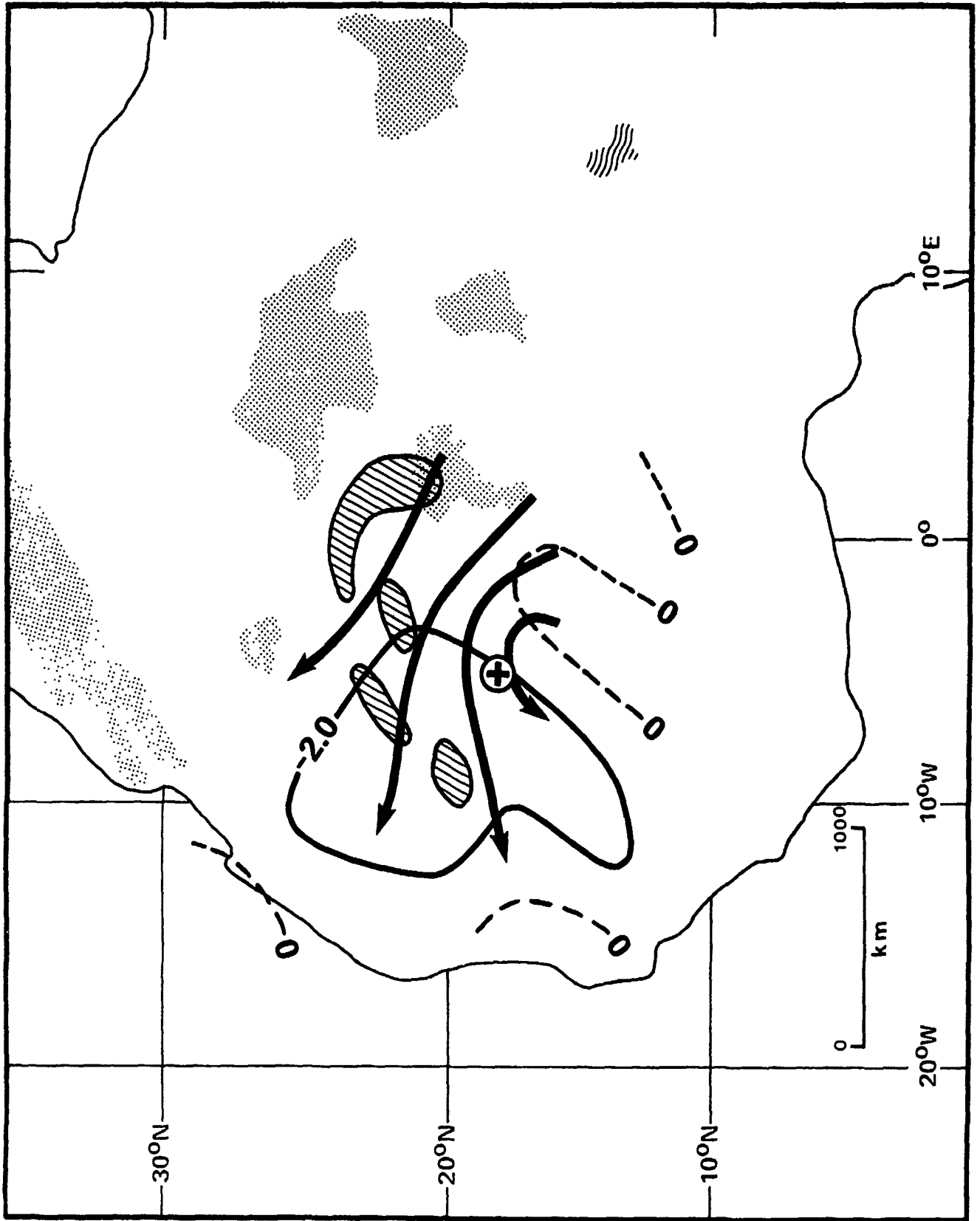


Figure 30

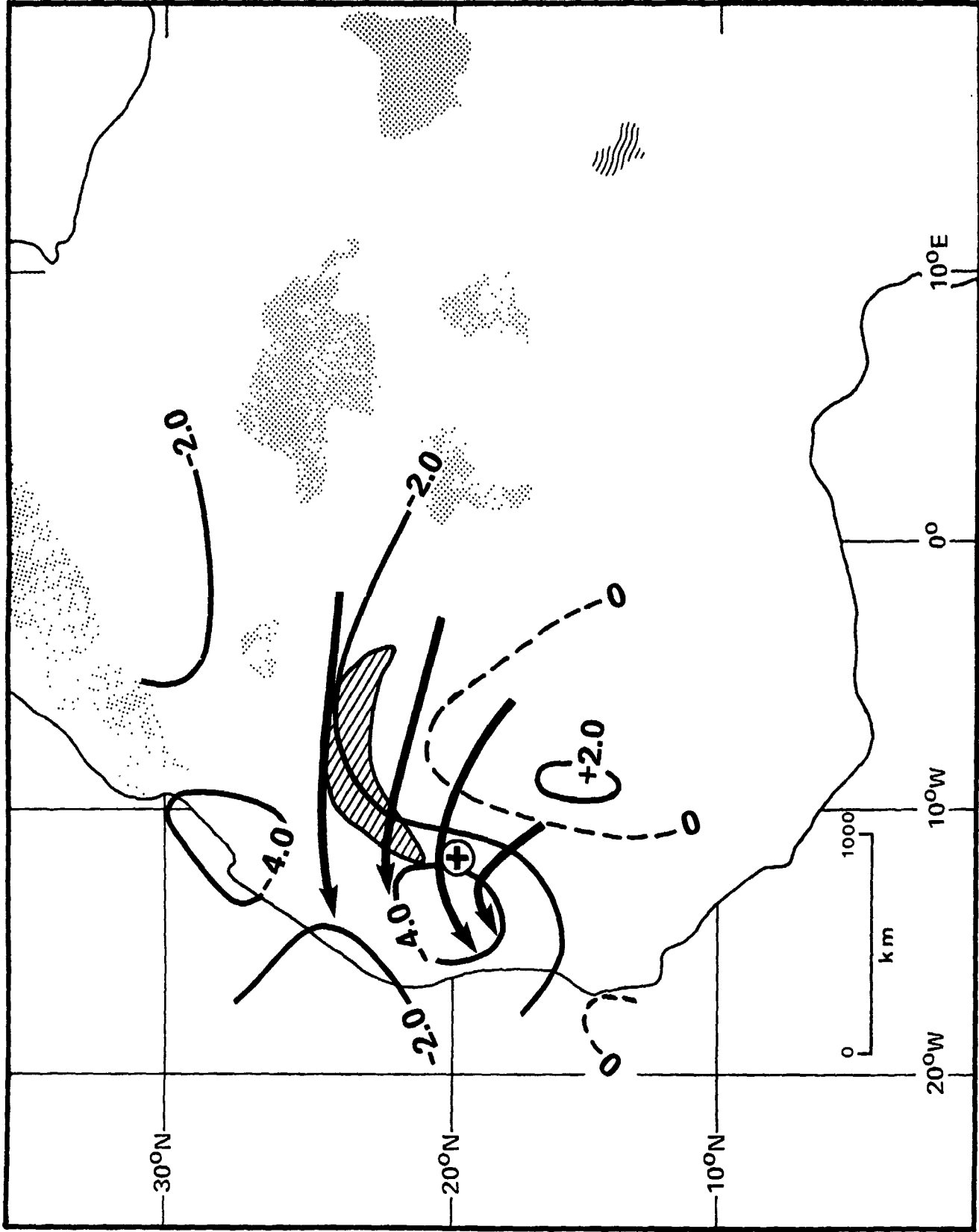


Figure 31

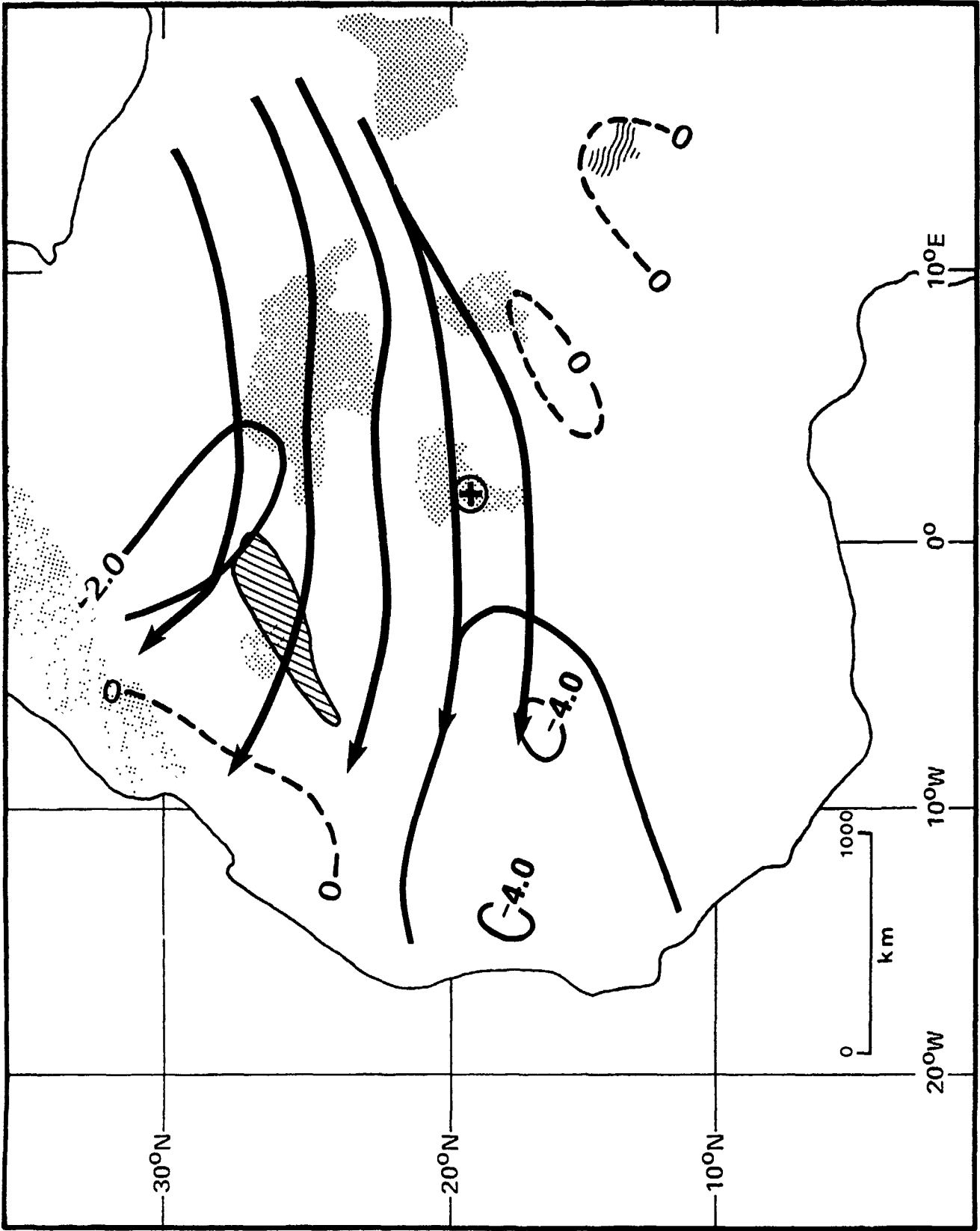


Figure 32

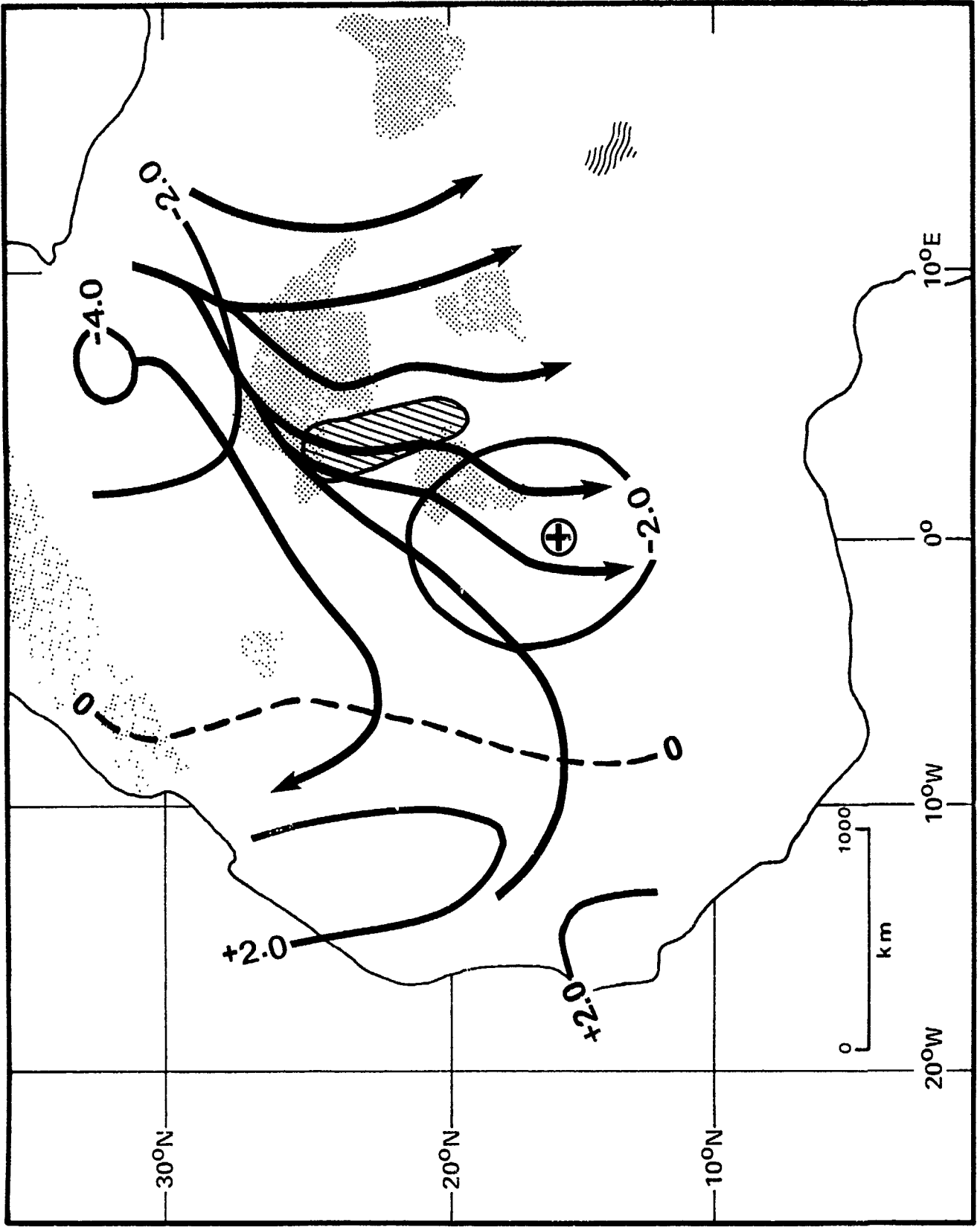


Figure 33

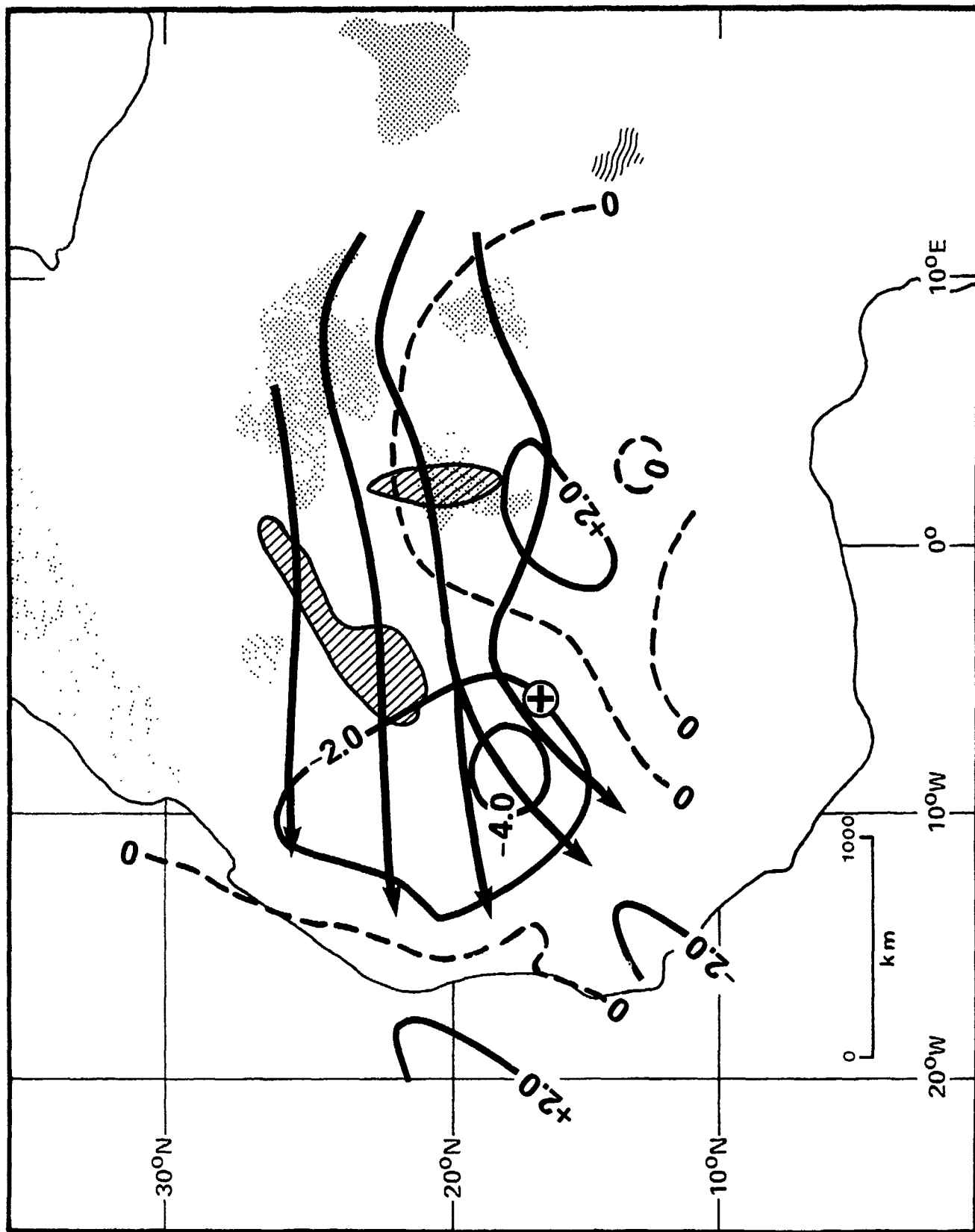


Figure 34

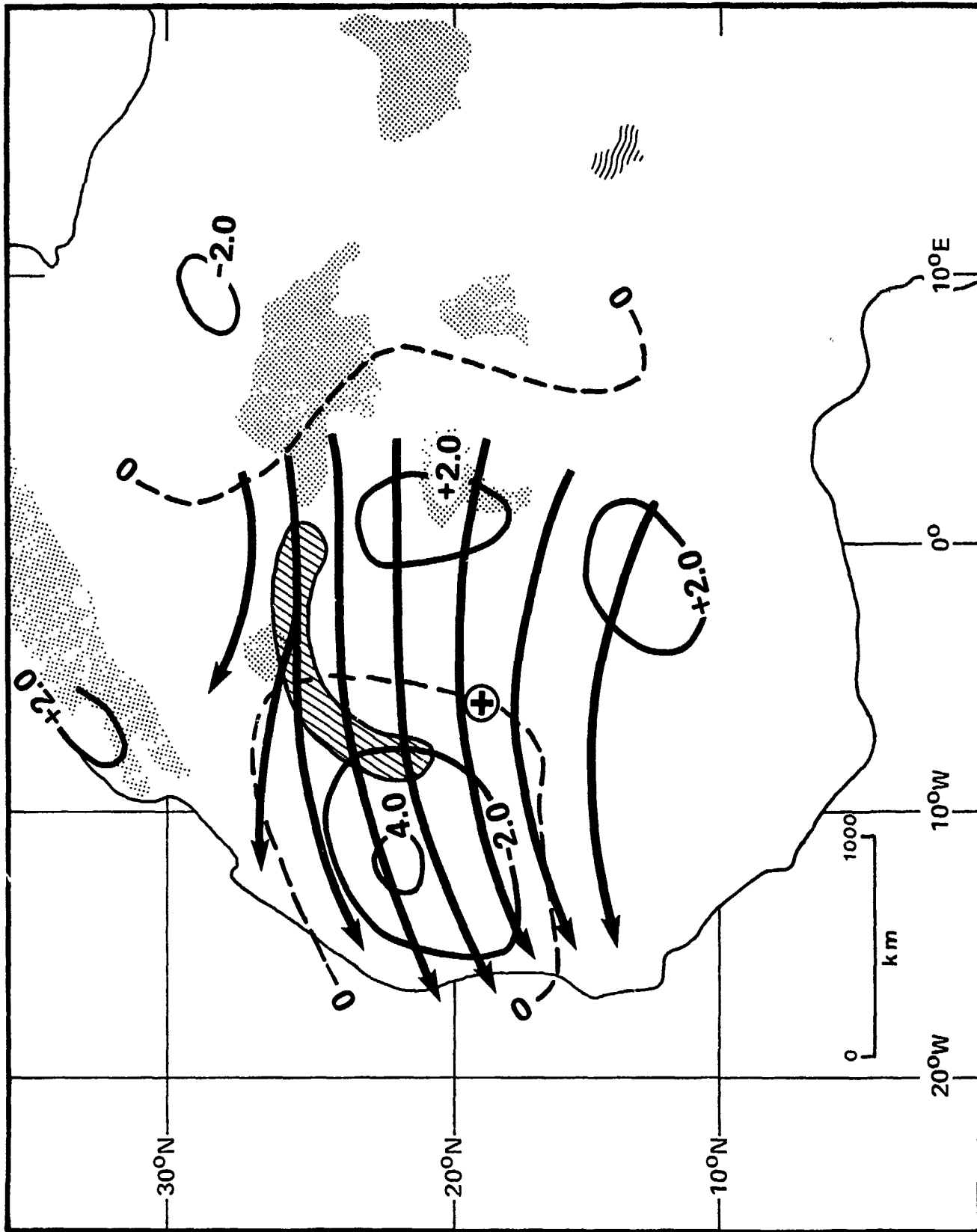


Figure 35

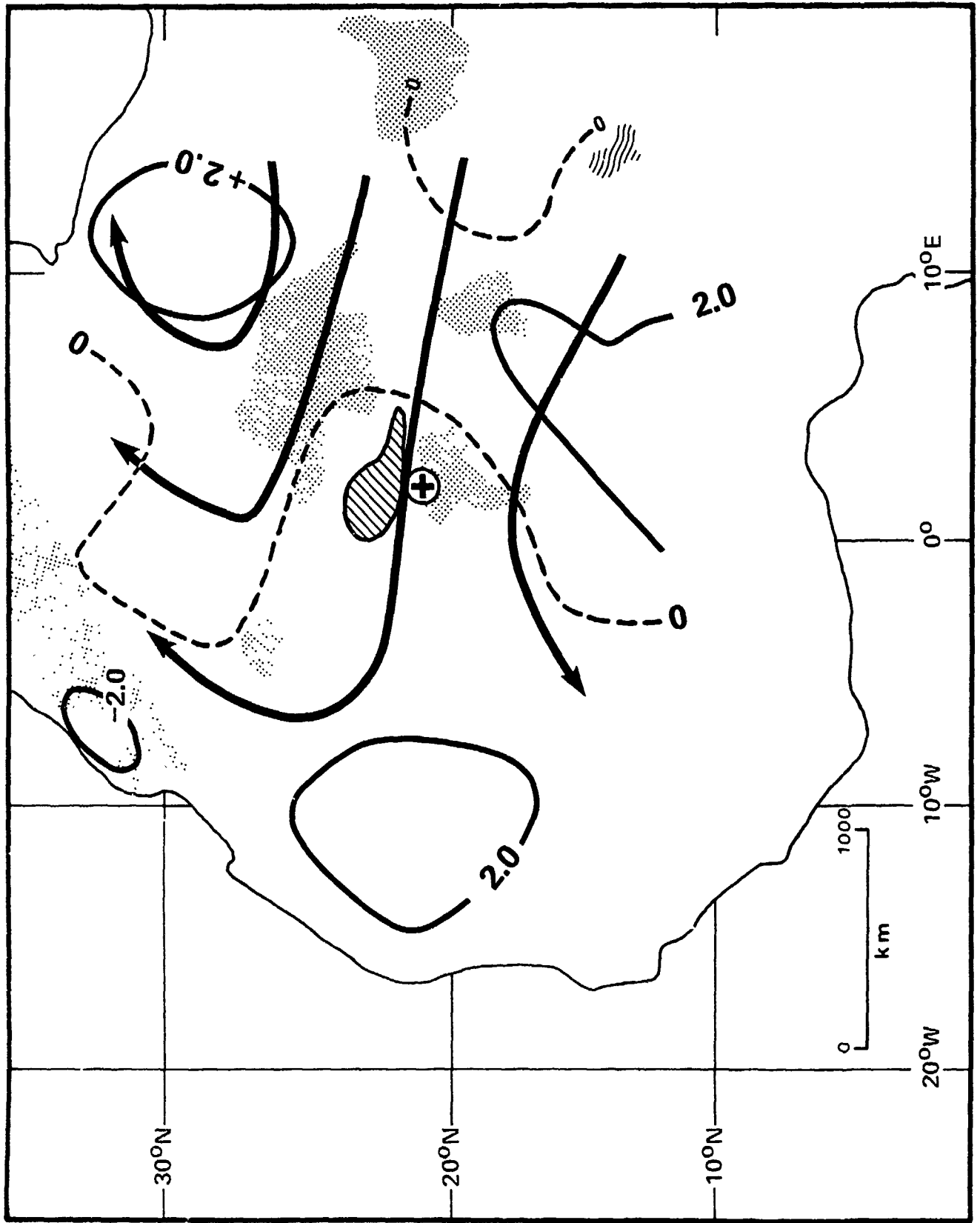


Figure 36

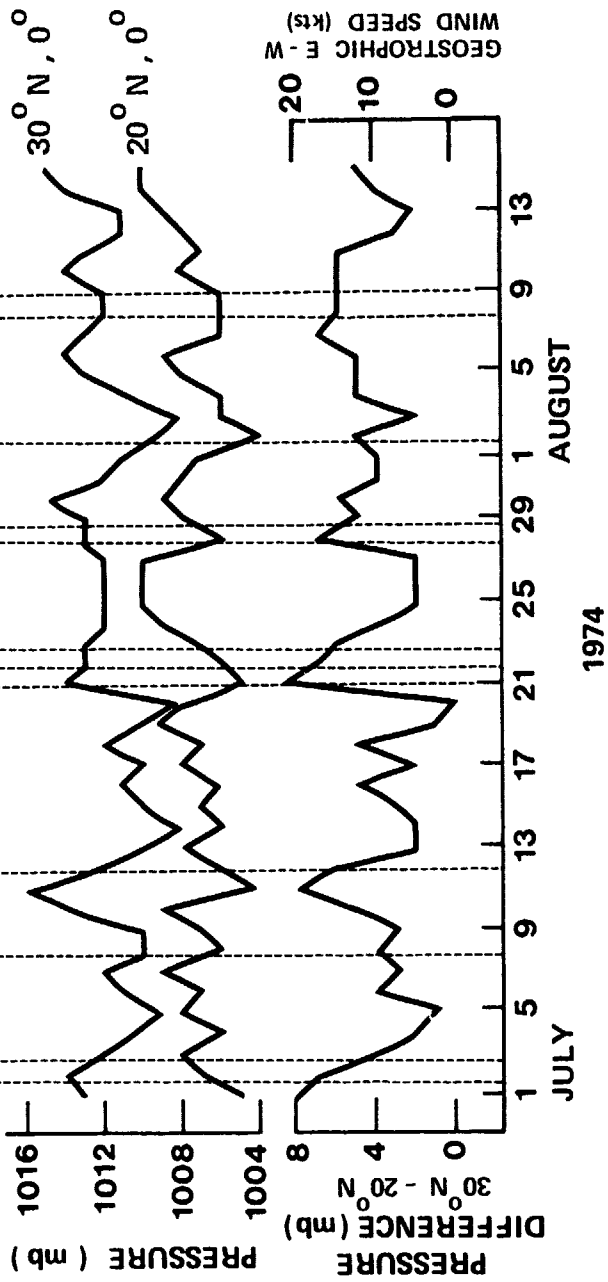


Figure 37

